Atmos. Chem. Phys., 15, 715–736, 2015
www.atmos-chem-phys.net/15/715/2015/
doi:10.5194/acp-15-715-2015

Atmospheric Chemistry and Physics
Open Access

Top-down estimates of European CH_4 and N_2O emissions based on four different inverse models

P. Bergamaschi[1], M. Corazza[1,a], U. Karstens[2], M. Athanassiadou[3], R. L. Thompson[4,b], I. Pison[4], A. J. Manning[3], P. Bousquet[4], A. Segers[1,c], A. T. Vermeulen[5,d], G. Janssens-Maenhout[1], M. Schmidt[4,e], M. Ramonet[4], F. Meinhardt[6], T. Aalto[7], L. Haszpra[8,9], J. Moncrieff[10], M. E. Popa[2,f], D. Lowry[11], M. Steinbacher[12], A. Jordan[2], S. O'Doherty[13], S. Piacentino[14], and E. Dlugokencky[15]

[1]European Commission Joint Research Centre, Institute for Environment and Sustainability, Ispra, Italy
[2]Max-Planck-Institute for Biogeochemistry, Jena, Germany
[3]Met Office, Exeter, UK
[4]Laboratoire des Sciences du Climat et de l' Environnement (LSCE), Gif sur Yvette, France
[5]Energy Research Centre of the Netherlands (ECN), Petten, the Netherlands
[6]Umweltbundesamt, Messstelle Schauinsland, Kirchzarten, Germany
[7]Finnish Meteorological Institute (FMI), Helsinki, Finland
[8]Hungarian Meteorological Service, Budapest, Hungary
[9]Research Centre for Astronomy and Earth Sciences, Geodetic and Geophysical Institute, Sopron, Hungary
[10]School of GeoSciences, The University of Edinburgh, Edinburgh, UK
[11]Dept. of Earth Sciences, Royal Holloway, University of London (RHUL), Egham, UK
[12]Swiss Federal Laboratories for Materials Science and Technology (Empa), Dübendorf, Switzerland
[13]Atmospheric Chemistry Research Group, University of Bristol, Bristol, UK
[14]Italian National Agency for New Technologies, Energy and Sustainable Development (ENEA), Rome, Italy
[15]NOAA Earth System Research Laboratory, Global Monitoring Division, Boulder, CO, USA
[a]now at: Agenzia Regionale per la Protezione dell'Ambiente Ligure, Genoa, Italy
[b]now at: Norwegian Institute for Air Research (NILU), Kjeller, Norway
[c]now at: Netherlands Organisation for Applied Scientific Research (TNO), Utrecht, the Netherlands
[d]now at: Dept. of Physical Geography and Ecosystem Science, Lund University, Lund, Sweden
[e]now at: Institut für Umweltphysik, Heidelberg, Germany
[f]now at: Institute for Marine and Atmospheric Research Utrecht, Utrecht University, Utrecht, the Netherlands

Correspondence to: P. Bergamaschi (peter.bergamaschi@jrc.ec.europa.eu)

Received: 11 March 2014 – Published in Atmos. Chem. Phys. Discuss.: 16 June 2014
Revised: 12 November 2014 – Accepted: 22 November 2014 – Published: 19 January 2015

Abstract. European CH_4 and N_2O emissions are estimated for 2006 and 2007 using four inverse modelling systems, based on different global and regional Eulerian and Lagrangian transport models. This ensemble approach is designed to provide more realistic estimates of the overall uncertainties in the derived emissions, which is particularly important for verifying bottom-up emission inventories.

We use continuous observations from 10 European stations (including 5 tall towers) for CH_4 and 9 continuous stations for N_2O, complemented by additional European and global discrete air sampling sites. The available observations mainly constrain CH_4 and N_2O emissions from north-western and eastern Europe. The inversions are strongly driven by the observations and the derived total emissions of larger countries show little dependence on the emission inventories used a priori.

Three inverse models yield 26–56 % higher total CH_4 emissions from north-western and eastern Europe compared

to bottom-up emissions reported to the UNFCCC, while one model is close to the UNFCCC values. In contrast, the inverse modelling estimates of European N_2O emissions are in general close to the UNFCCC values, with the overall range from all models being much smaller than the UNFCCC uncertainty range for most countries. Our analysis suggests that the reported uncertainties for CH_4 emissions might be underestimated, while those for N_2O emissions are likely overestimated.

1 Introduction

Atmospheric methane (CH_4) and nitrous oxide (N_2O) are the second and third most important long-lived anthropogenic greenhouse gases (GHGs), after carbon dioxide (CO_2). CH_4 and N_2O have large global warming potentials of 28 and 265, respectively, relative to CO_2 over a 100-year time horizon (Myhre et al., 2013). Globally averaged dry-air mole fractions of CH_4 reached 1819 ± 1 ppb in 2012, 160 % above the pre-industrial level (1750) of ~ 700 ppb, while N_2O reached 325.1 ± 0.1 ppb, ~ 20 % higher than pre-industrial level (270 ppb) (WMO, 2013). CH_4 and N_2O contributed ~ 18 % and ~ 6 %, respectively, to the direct anthropogenic radiative forcing of all long-lived GHGs in 2012, relative to 1750 (NOAA Annual Greenhouse Gas Index (AGGI), http://www.esrl.noaa.gov/gmd/aggi/). CH_4 also has significant additional indirect radiative effects due to its feedback on global OH concentrations, tropospheric ozone, and stratospheric water vapour, and the generation of CO_2 as the final product of the CH_4 oxidation chain (Forster et al., 2007; Shindell et al., 2005). These indirect effects are reflected in the CH_4 emission-based radiative forcing of 0.97 (0.74 to 1.20) Wm^{-2}, which is about twice the concentration-based radiative forcing of 0.48 (0.43 to 0.53) Wm^{-2} (Myhre et al., 2013). In addition to its significant contribution to global warming, N_2O plays an important role in the depletion of stratospheric ozone, with its current ozone depletion potential-weighted emissions being the largest of all ozone-depleting substances (Ravishankara et al., 2009).

On the European scale, combined emissions of CH_4 and N_2O contributed 15.4 % to total GHG emissions (in CO_2-equivalents) reported under the United Nations Framework Convention on Climate Change (UNFCCC) by the EU-15 countries for 2012 (16.3 % for EU-28) (EEA, 2014). The large reductions of both CH_4 and N_2O emissions since 1990 (CH_4 by 33 %; N_2O by 34 %) reported by the EU-15 contributed significantly to the reduction of its total GHG emissions by 15.1 % (2012 compared to 1990).

GHG emissions reported to the UNFCCC are based on statistical activity data and source-specific and country-specific emission factors (IPCC, 2006). For CH_4 and N_2O however, such "bottom-up" emission inventories have considerable uncertainties, mainly due to the large variability of emission factors, which for many CH_4 and N_2O sources are not very well characterized (e.g. CH_4 emissions from landfills, gas production facilities and distribution networks, or N_2O emissions from agricultural soils (e.g. Karion et al., 2013; Leip et al., 2011)).

Complementarily to "bottom-up" approaches, emissions can be estimated using atmospheric measurements and inverse modelling. This "top-down" technique is widely used to estimate GHG emissions on the global and continental scale (e.g. Bergamaschi et al., 2013; Bousquet et al., 2006; Hein et al., 1997; Houweling et al., 1999; Kirschke et al., 2013; Mikaloff Fletcher et al., 2004a, b for CH_4 and Hirsch et al., 2006; Huang et al., 2008; Thompson et al., 2014 for N_2O). With the availability of quasi-continuous GHG measurements and the increasing number of regional monitoring stations, especially in Europe and North America, various inverse modelling studies have estimated emissions also on the regional to country scale (e.g. Bergamaschi et al., 2010; Corazza et al., 2011; Kort et al., 2008; Manning et al., 2011; Miller et al., 2013), demonstrating the potential of using such top-down methods for independent verification of bottom-up inventories (Bergamaschi, 2007). The use of atmospheric measurements and inverse modelling for verification has also been recognized by the IPCC (2006).

Currently, only anthropogenic GHG emissions are reported to UNFCCC. In many specific cases, such as the European CH_4 and N_2O emissions discussed in this study, the contribution of natural emissions is considered to be relatively small. Nevertheless, quantitative comparison between inverse modelling and bottom-up estimates also requires estimates of natural emissions.

A further challenge with inverse modelling, particularly for its use in verifying bottom-up estimates, is the provision of realistic uncertainties for the derived emissions. Although various studies attempt to take account of estimates of the model representation and transport errors, such estimates are typically based on strongly simplified assumptions. As a complementary approach, the range of results from an ensemble of models can be analysed and may be considered a more realistic estimate of the overall uncertainty, provided the applied models are largely independent and represent well the range of current models. Furthermore, detailed model comparisons, and verification with independent validation data, allow the model characteristics to be analysed in detail and potential model deficiencies to be identified. Comparisons of global inverse models have been performed for CO_2 (e.g. Peylin et al., 2013; Stephens et al., 2007), CH_4 (Kirschke et al., 2013) and N_2O (Thompson et al., 2014), focusing on the global and continental scale. Here, we present for the first time a detailed comparison of inverse models estimating European CH_4 and N_2O emissions. We use four inverse models, based on different global and regional Eulerian and Lagrangian transport models. The inversions are constrained by a comprehensive data set of quasi-continuous observations from European monitoring stations (including five

tall towers), complemented by further European and global discrete air sampling sites.

2 Atmospheric measurements

The European monitoring stations used in the CH_4 and N_2O inversions are summarized in Table 1. The monitoring stations include 10 sites with quasi-continuous measurements for CH_4 (i.e. providing data with hourly or higher time resolution), and 9 sites with quasi-continuous N_2O measurements. Five of these stations are equipped with tall towers (Cabauw, Bialystok, Ochsenkopf, Hegyhatsal, and Angus), with uppermost sampling heights above the surface by 97–300 m. The measurements at the tall towers were set up or improved within the EU project CHIOTTO ("Continuous High-precision Tall Tower Observations") (Popa et al., 2010; Thompson et al., 2009; Vermeulen et al., 2007, 2011). Additional quasi-continuous measurements are from the AGAGE (Advanced Global Atmospheric Gases Experiment) network (Cunnold et al., 2002; Rigby et al., 2008) at Mace Head, from the operational network of the German Federal Environment Agency (UBA) at Schauinsland, from the Finnish Meteorological Institute at Pallas (Aalto et al., 2007), from the Swiss Federal Laboratories for Materials Science and Technology (EMPA) at Jungfraujoch, and from the Royal Holloway University of London (RHUL) in London. Furthermore, we use CH_4 and N_2O discrete air samples from the NOAA Earth System Research Laboratory (ESRL) global cooperative air sampling network at 10 European sites (and for the global inverse models, additional global NOAA sites) (Dlugokencky et al., 1994, 2003, 2009), and CH_4 discrete air samples from the French RAMCES (Réseau Atmosphérique de Mesure des Composés à Effet de Serre) network (Schmidt et al., 2006) at 5 European sites. Finally, discrete air samples from the Max-Planck-Institute for Biogeochemistry at the Shetland Islands, and from the Italian National Agency for New Technologies, Energy and Sustainable Development (ENEA) at Lampedusa were used. Both quasi-continuous and discrete air sample measurements are based on gas chromatography (GC) using flame ionization detectors (FIDs) for CH_4, and electron capture detectors (ECDs) for N_2O. Measurements are reported as dry air mole fractions (nmol mol^{-1}, abbreviated as ppb).

For CH_4, we generally apply the NOAA04 CH_4 standard scale (Dlugokencky et al., 2005). AGAGE CH_4 data were converted to NOAA04 using a scaling factor of 1.0003 (Prinn et al., 2000), and RAMCES CH_4 data were scaled by 1.0124 from CMDL83 to NOAA04 (Dlugokencky et al., 2005). CH_4 comparisons of high-pressure cylinders performed in the frame of the European projects MethMoniteur, IMECC, Geomon and CHIOTTO, and WMO between 2004 and 2010 showed that the CH_4 measurements of the CHIOTTO, NOAA, RAMCES, UBA, and RHUL networks agreed within 2 ppb. Furthermore, comparison of the quasi-continuous measurements at Pallas, Mace Head, Ochsenkopf, and Hegyhatsal with NOAA discrete air samples (using measurements coinciding within 1 h, and the additional condition that the quasi-continuous measurements show low variability within a 5 h time window) showed annual average absolute CH_4 biases of less than 4 ppb during 2006 and 2007, the target period of this study.

While the merged CH_4 data set used in this study can, therefore, be considered reasonably consistent, this is not the case for N_2O, for which significant offsets are apparent between different monitoring laboratories, even though most laboratories use N_2O primary standards from NOAA/ESRL. These offsets exceed the compatibility goal of ± 0.1 ppb (1σ) recommended by WMO GAW (WMO, 2012) (Table 7). We, therefore, adopt the approach developed by Corazza et al. (2011) to correct for these calibration offsets in the inversion (see also Sect. 3), using the NOAA discrete air samples (which are reported on the NOAA-2006 scale; Hall et al., 2007) as a common reference. Corazza et al. (2011) showed that the N_2O bias correction derived in the inversion agreed within 0.1–0.2 ppb (N_2O dry-air mole fraction) with the bias derived from the comparison of quasi-continuous measurements with parallel NOAA discrete air samples. We emphasize that this bias correction assumes that the bias remains constant during the inversion period (yearly for TM5) and, therefore, cannot correct for changes of the systematic bias on shorter timescales.

For validation, CH_4 measurements of discrete air samples from three European aircraft profile sites in Scotland, France, and Hungary are used, operated within the European CarboEurope project. The analyses of these samples were performed at LSCE, in the same manner as the RAMCES surface measurements.

3 Modelling

3.1 Modelling protocol

The modelling protocol used in this study prescribed mainly the basic settings for the inversions, such as a priori emission inventories, observational data sets, time period, and requested model output. Atmospheric sinks were not prescribed. For both CH_4 and N_2O, two types of inversions were performed: (1) the base inversions, S1–CH_4 and S1–N_2O, respectively, using detailed bottom-up emission inventories for anthropogenic and natural sources as a priori emission estimates, and (2) the "free inversions", S2–CH_4 and S2–N_2O, which do not use these bottom-up inventories. The objective of these "free inversions" is to explore the information content of the observations in the absence of detailed a priori information.

The CH_4 and N_2O emission inventories applied in S1–CH_4 and S1–N_2O are summarized in Tables 3 and 4, respectively. For the anthropogenic sources (except biomass burning), the EDGARv4.1 emission inventory for 2005 was used

Table 1. European atmospheric monitoring stations used in the inversions (2006–2007). "ST" specifies the sampling type ("CM": quasi-continuous measurements, providing data with hourly time resolution; "FM": discrete air measurements with typically weekly sampling frequency). "CH_4" and "N_2O" indicate which stations have been used in the CH_4 and N_2O inversions, respectively.

ID	Station name	Data provider	Latitude	Longitude	Altitude	ST	CH_4	N_2O
					m a.s.l.			
PAL	Pallas, Finland	FMI	67.97	24.12	560	CM	•	•
		NOAA				FM	•	•
STM	Ocean station M, Norway	NOAA	66.00	2.00	5	FM	•	•
ICE	Heimay, Vestmannaeyjar, Iceland	NOAA	63.34	−20.29	127	FM	•	•
SIS	Shetland Island, UK	MPI-BGC	59.85	−1.27	46	FM	•	•
TT1	Angus, UK (222 m level)	CHIOTTO	56.55	−2.98	535	CM	•	•
BAL	Baltic Sea, Poland	NOAA	55.35	17.22	28	FM	•	•
MHD	Mace Head, Ireland	AGAGE	53.33	−9.90	25	CM	•	•
		NOAA				FM	•	•
BI5	Bialystok, Poland (300 m level)	CHIOTTO	53.23	23.03	460	CM	•	•
CB3	Cabauw, Netherlands (120 m level)	CHIOTTO	51.97	4.93	118	CM	•	•
LON	Royal Holloway, London, UK	RHUL	51.43	−0.56	45	CM	•	
OX3	Ochsenkopf, Germany (163 m level)	CHIOTTO	50.05	11.82	1185	CM	•	•
		NOAA				FM	•	•
LPO	Ile Grande, France	RAMCES	48.80	−3.58	30	FM	•	
GIF	Gif sur Yvette, France	RAMCES	48.71	2.15	167	FM	•	
SIL	Schauinsland, Germany	UBA	47.91	7.91	1205	CM	•	•
HPB	Hohenpeissenberg, Germany	NOAA	47.80	11.01	985	FM	•	•
HU1	Hegyhatsal, Hungary (96 m level)	CHIOTTO	46.95	16.65	344	CM	•	•
		NOAA				FM	•	•
JFJ	Jungfraujoch, Switzerland	EMPA	46.55	7.98	3580	CM	•	•
PUY	Puy de Dome, France	RAMCES	45.77	2.97	1475	FM	•	
BSC	Black Sea, Constanta, Romania	NOAA	44.17	28.68	3	FM	•	•
PDM	Pic du Midi, France	RAMCES	42.94	0.14	2887	FM	•	
BGU	Begur, Spain	RAMCES	41.97	3.23	15	FM	•	
LMP	Lampedusa, Italy	ENEA	35.52	12.63	45	FM	•	
		NOAA				FM		•

Table 2. Atmospheric models.

Model	Institution	Resolution of transport model: Horizontal	Vertical	Meteorology
TM5-4DVAR	EC JRC	Europe: $1^\circ \times 1^\circ$ Global: $6^\circ \times 4^\circ$	25	ECMWF ERA-INTERIM
LMDZ-4DVAR	LSCE	Europe: $\sim 1.2^\circ \times 0.8^\circ$ Global: $\sim 7^\circ \times 3.6^\circ$	19	Nudged to ECMWF ERA-INTERIM
TM3-STILT	MPI-BGC	Europe: $0.25^\circ \times 0.25^\circ$[a] (STILT) Global: $5^\circ \times 4^\circ$ (TM3)	61 (STILT) 19 (TM3)	ECMWF operational analysis (STILT) NCEP reanalysis (TM3)
NAME-INV	Met Office	$0.56^\circ \times 0.37^\circ$[b]	31[c]	Met Office Unified Model (UM)

[a] Horizontal resolution of inversion: $1^\circ \times 1^\circ$.
[b] Horizontal resolution of inversion: $0.42^\circ \times 0.27^\circ$.
[c] 31 levels from surface to 19 km.

(as 2005 is the most recent available year in EDGARv4.1). For S2–CH_4 and S2–N_2O, a homogeneous distribution of emissions over land and over the ocean was used as starting point for the optimization (i.e. a "weak a priori" for TM5-4DVAR and TM3-STILT), with global total CH_4 and N_2O emissions over land and over the ocean, respectively, close to the total emissions over land and over the ocean of the detailed a priori inventories (Bergamaschi et al., 2010; Corazza et al., 2011), hence effectively limiting the emissions that can be attributed to the ocean. For the NAME-INV model, no separation was made between land and ocean. Moreover, the NAME-INV model started from random emission maps rather than a homogeneous distribution of emissions. Inversions S2 were not available for LMDZ-4DVAR.

For the European limited domain models NAME-INV and STILT, background CH_4 and N_2O mixing ratios were calcu-

Table 3. CH_4 emission inventories used as a priori in inversion S1–CH_4.

Source	Inventory	Global total $Tg\,CH_4\,yr^{-1}$
Anthropogenic		
Coal mining	EDGARv4.1[a]	40.3
Oil production and refineries	EDGARv4.1[a]	26.1
Gas production and distribution	EDGARv4.1[a]	46.8
Enteric fermentation	EDGARv4.1[a]	96.9
Manure management	EDGARv4.1[a]	11.3
Rice cultivation	EDGARv4.1[a]	34.0
Solid waste	EDGARv4.1[a]	28.1
Waste water	EDGARv4.1[a]	30.0
Further anthropogenic sources[b]	EDGARv4.1[a]	16.9
Biomass burning	GFEDv2 (van der Werf et al., 2004)	19.7–20.2[c]
Natural		
Wetlands	Inventory of J. Kaplan (Bergamaschi et al., 2007)	175.0
Wild animals	(Houweling et al., 1999)	5.0
Termites	(Sanderson, 1996)	19.3
Ocean	(Lambert and Schmidt, 1993)	17.0
Soil sink	(Ridgwell et al., 1999)	−37.9
Total		528.4–528.9[d]

[a] EDGARv4.1 CH_4 emissions for 2005.
[b] Including CH_4 emission from transport, residential sector, energy manufacturing and transformation, industrial processes and product use, and agricultural waste burning.
[c] GFEDv2 CH_4 emissions for 2006 and 2007, respectively.
[d] Global total CH_4 emissions for 2006 and 2007, respectively.

Table 4. N_2O emission inventories used as a priori in inversion S1–N_2O.

Source	Inventory	Global total $Tg\,N_2O\,yr^{-1}$
anthropogenic		
Agricultural soils	EDGARv4.1[a]	4.5
Indirect N_2O emissions	EDGARv4.1[a]	1.6
Manure management	EDGARv4.1[a]	0.3
Transport	EDGARv4.1[a]	0.3
Residential	EDGARv4.1[a]	0.3
Industrial processes and product use	EDGARv4.1[a]	0.6
Energy manufacturing and transformation	EDGARv4.1[a]	0.3
Waste	EDGARv4.1[a]	0.4
Further anthropogenic sources[b]	EDGARv4.1[a]	0.1
Biomass burning	GFEDv2 (van der Werf et al., 2004)	1.0–1.1[c]
Post-forest clearing enhanced	(Bouwman et al., 1995)	0.6
Natural		
Natural soils	(Bouwman et al., 1995)	7.2
Ocean	(Bouwman et al., 1995)	5.7
Total		22.7–22.8[d]

[a] EDGARv4.1 N_2O emissions for 2005.
[b] Including N_2O emission from agricultural waste burning, and oil and gas sector.
[c] GFEDv2 N_2O emissions for 2006 and 2007, respectively.
[d] Global total N_2O emissions for 2006 and 2007, respectively.

lated by TM5-4DVAR (for NAME-INV CH_4 and N_2O inversions and STILT N_2O inversions) and by TM3 (for STILT CH_4 inversions) following the two-step scheme of Rödenbeck et al. (2009).

All models used the same observational data set described in Sect. 2 (with the exception of a few stations that are outside the domain of the limited domain models). For the continuously operated monitoring stations in the boundary layer, measurements between 12:00 and 15:00 LT were assimilated, when measurements (and model simulations) are usually representative of large regions and much less affected by local emissions. In contrast, for mountain sites night-time measurements (between 00:00 and 03:00 LT) were used to avoid the potential influence of upslope transport on the measurements, which is frequently observed at mountain stations during daytime. Different from this sampling scheme (applied in TM5-4DVAR, LMDZ-4DVAR, and TM3-STILT), the NAME-INV model used observations at all times, but with local contributions excluded as in Manning et al. (2011).

For the N_2O inversions, bias corrections for the N_2O observations from different networks or institutes were calculated within the 4DVAR optimization of the TM5-4DVAR and LMDZ-4DVAR models, as described by Corazza et al. (2011). For NAME-INV and TM3-STILT, the bias corrections calculated by TM5-4DVAR (Table 7) were applied.

3.2 Atmospheric models

The atmospheric models used in this study are summarized in Table 2 and briefly described in the following.

3.2.1 TM5-4DVAR

The TM5-4DVAR inverse modelling system is described in detail by Meirink et al. (2008). It is based on the two-way nested atmospheric zoom model TM5 (Krol et al., 2005). In this study we apply the zooming with $1° \times 1°$ resolution over Europe, while the global domain is simulated at a horizontal resolution of 6° (longitude) × 4° (latitude). TM5 is an offline transport model, driven by meteorological fields from the European Centre for Medium-Range Weather Forecasts (ECMWF) ERA-Interim reanalysis (Dee et al., 2011). The 4-dimensional variational (4DVAR) optimization technique minimizes iteratively a cost function using the adjoint of the tangent linear model and the m1qn3 algorithm for minimization (Gilbert and Lemaréchal, 1989). We apply a "semi-exponential" description of the probability density function for the a priori emissions to force the a posteriori emissions to remain positive (Bergamaschi et al., 2009, 2010). In inversion S1–CH_4, four groups of CH_4 emissions are optimized independently: (1) wetlands, (2) rice, (3) biomass burning, and (4) all remaining sources (Bergamaschi et al., 2010). For S1–N_2O the following four groups of N_2O emissions are optimized: (1) soil, (2) ocean, (3) biomass burning, and (4) all remaining emissions (Corazza et al., 2011). In S2–CH_4 and S2–N_2O, only total emissions are optimized. We assume uncertainties of 100 % per grid-cell and month for each source group and apply spatial correlation scale lengths of 200 km in S1–CH_4 and S1–N_2O. In the "free inversions" S2–CH_4 and S2–N_2O, smaller correlation scale lengths of 50 km, and larger uncertainties of 500 % per grid-cell and month are used to give the inversion enough freedom to retrieve regional hot spots (Bergamaschi et al., 2010; Corazza et al., 2011). The temporal correlation timescales are set to zero for the source groups with significant seasonal variations, and 9.5 months for the "remaining" CH_4 and N_2O sources (which include major anthropogenic sources that are assumed to have no or only small seasonal variations) in S1–CH_4 and S1–N_2O, and 1 month for the total emissions optimized in S2–CH_4 and S2–N_2O.

The photochemical sinks of CH_4 (due to OH in the troposphere, and OH, Cl, and $O(^1D)$ in the stratosphere) are simulated as described in Bergamaschi et al. (2010). The stratospheric sinks of N_2O (photolysis and reaction with excited oxygen $O(^1D)$) are modelled as in Corazza et al. (2011).

The observation errors were set to 3 ppb for CH_4, and 0.3 ppb for N_2O. The model representation error is estimated as a function of local emissions and 3-D gradients of simulated mixing ratios (Bergamaschi et al., 2010), resulting in overall (combined measurement and model representation) errors in the range between 3 ppb and up to $\sim$ 1 ppm for CH_4, and between 0.3 ppb and up to several ppb for N_2O. For the N_2O inversions we optimize bias parameters for the N_2O observations from different networks or institutes (see Table 7), as described by Corazza et al. (2011).

3.2.2 LMDZ-4DVAR

The LMDZ-4DVAR inverse modelling framework is based on the offline and adjoint models of the Laboratoire de Météorologie Dynamique, version 4 (LMDZ) general circulation model (Hourdin and Armengaud, 1999; Hourdin et al., 2006). The offline model is driven by archived fields of winds, convection mass fluxes, and planetary boundary layer (PBL) exchange coefficients that have been calculated in prior integrations of the complete general circulation model, which was nudged to ECMWF ERA-Interim winds (Dee et al., 2011). In this study, LMDZ is used with a zoom over Europe at a resolution of approximately $1.2° \times 0.8°$ and decreasing resolution away from Europe to a maximum grid size of approximately $7.2° \times 3.6°$. LMDZ has 19 hybrid pressure levels in the vertical dimension. The optimal fluxes were found by solving the cost function using the adjoint model and the Lanczos algorithm for N_2O and the m1qn3 algorithm for CH_4.

Details about the inversion framework for CH_4 are given in Pison et al. (2009, 2013). Only the total net emissions of methane are optimized, at the resolution of the grid-cell for 8-day periods. Prior uncertainties in each grid-cell are set to 100 % of the maximum flux over the grid-cell and its

eight neighbours (so as to allow for a misplacement of the sources). Correlation scale lengths are used to compute the off-diagonal terms in the error covariance matrix: they are set at 500 km on land and 1000 km on sea (land and sea are not correlated); there are no time correlations. The "observation" errors include the estimates of the errors due to the transport model and to the representativity of the grid-cell compared to the measurement (combined measurement and model error ranging between 3 ppb and up to 450 ppb). Note that the OH fields are inverted simultaneously to the methane emissions, with constraints from methyl-chloroform (Pison et al., 2009; 2013).

Details about the inversion framework for N_2O can be found in Thompson et al. (2011). For N_2O, only total emissions were optimized. Prior uncertainties in each grid-cell were set to 100 % and correlation scale lengths of 500 km over land, 1000 km over ocean, and 3 months were used to form the full error covariance matrix, which was subsequently scaled to be consistent with a global total uncertainty of 3 TgN yr^{-1} (approximately 18 %). The error of the N_2O observations was set to 0.3 ppb. Model representation errors incorporated an estimate of aggregation error, i.e. distribution of emissions within the grid-cell (Bergamaschi et al., 2010), and horizontal advection errors (Rödenbeck et al., 2003), resulting in total model errors ranging from about 0.2 ppb to 1 ppb. In addition to the emissions, bias parameters for the N_2O observations from different networks or institutes were optimized, similarly to TM5-4DVAR (Corazza et al., 2011).

3.2.3 TM3-STILT

In the Jena inversions, the coupled system TM3-STILT is used for regional-scale high-resolution inversions. TM3-STILT (Trusilova et al., 2010) is a combination of the coarse-grid global 3-dimensional atmospheric offline transport model TM3 (Heimann and Koerner, 2003) and the fine-scale regional Stochastic Time-Inverted Lagrangian Transport model STILT (Gerbig et al., 2003; Lin et al., 2003). The models are coupled using the two-step nesting scheme of Rödenbeck et al. (2009), which allows the use of completely independent models for the representation of the global and the regional transport. The variational inversion algorithm of the Jena inversion scheme, applied in the global as well as in the regional inversion step, is described in detail in Rödenbeck (2005). In this study, the global transport model TM3 is used with a spatial resolution of $4^\circ \times 5^\circ$ and 19 vertical levels. STILT is driven by meteorological fields from ECMWF operational analysis, used here with a spatial resolution of $0.25^\circ \times 0.25^\circ$ and confined to the lowest 61 vertical layers. The regional TM3-STILT inversions are conducted in this study on a $1^\circ \times 1^\circ$ horizontal resolution grid covering the greater part of Europe (12° W–35° E, 35–62° N). Regional inversion results for CH_4 were obtained directly by the TM3-STILT system. For the regional N_2O inversions the same modular nesting technique is applied to couple STILT with a baseline provided by TM5-4DVAR (Bergamaschi et al., 2010; Corazza et al., 2011) and the regional inversion step is performed in the Jena inversion system. The latter combination is referred to as TM5-STILT in the presentation of the N_2O inversion results. In all regional inversions we optimize the total emissions. Uncertainties of 100 % per grid-cell and month, with a spatial correlation scale length of 600 km and a temporal correlation timescale of 1 month, are assumed in the regional S1–CH_4 and S1–N_2O inversions. In both S2 inversions the uncertainties are set to 500 % with a correlation scale length of 60 km and correlation timescale of 1 month. The observation errors were set to 3 ppb for CH_4 and 0.2 ppb for N_2O. Model representation errors are assigned to the individual sites according to their location with respect to continental, remote or oceanic situations (Rödenbeck, 2005), resulting in overall (combined measurement and model representation) errors in the range of 10–30 ppb for CH_4, and 0.8 and 2.4 ppb for N_2O. For N_2O the bias parameters estimated by TM5-4DVAR (see Table 7) are applied in the regional inversions.

3.2.4 NAME-INV

The NAME-INV inverse modelling system is described in Manning et al. (2011) using one station to estimate UK and Northern European emissions of various trace gases and in Athanassiadou et al. (2011) for multiple stations across Europe. The transport of CH_4 and N_2O from sources to observations is performed using the UK Met Office Lagrangian model NAME (Jones et al., 2007). Thousands of particles are released from each measurement for each 2 h period in 2006 and 2007, and these are tracked backwards in time over a period of 13 days (long enough for the majority of particles to leave the domain of interest). The 13-day time-integrated concentrations only include contributions from 0 to 100 m a.g.l., representative of surface emissions. The meteorological fields needed to run NAME are from the global version of the Met Office Unified Model (UM) at a resolution of $0.56^\circ \times 0.37^\circ$ and 31 vertical levels from surface to about 19 km (see Table 2). The domain used for the inversion extends from 14.63° W to 39.13° E and from 33.81° N to 72.69° N, with a resolution of $0.42^\circ \times 0.27^\circ$ in the longitudinal and latitudinal directions respectively. The inversion is initialized either from the modelling protocol a priori or from a random emissions field as in Manning et al. (2011). In the latter case, the cost function used in the optimization is the same as in Manning et al. (2011). In S1, when the inversion is initialized and guided by the a priori emission inventory, a modified version is used (original cost function + root mean square error (RMSE) between modelled values and a priori). To account for the imbalance in the contribution from different grid boxes (i.e. the grids more distant from the observations are expected to contribute less than those that are closer), grid boxes are progressively grouped together

into increasingly larger boxes as the individual contributions decrease.

In all inversions, the total annual emissions are optimized without any partitioning to various sectors. The background values used for CH_4 and N_2O are from TM5-4DVAR following the two-step scheme of Rödenbeck et al. (2009). Observations at all times have been used (i.e. not only in the time windows specified in Sect. 3.1), but excluding local contributions (Manning et al., 2011). An estimate of the uncertainty in the emissions is obtained from the 5th and 95th percentiles of 52 independent inversion solutions (the mean of these being the final solution). The independent inversion solutions are considered to simulate uncertainties in the meteorology, dispersion and observations. For each inversion a different time series of random noise is applied to the observations. The random element at each observation is multiplicative and taken from a lognormal distribution with mean 1 and variance, arbitrarily, set to one fifth of the standard deviation of baseline observations about a smoothed baseline value as in Manning et al. (2011). For this project the baseline standard deviation values 9.5 ppb (CH_4) and 0.194 ppb (N_2O) were used.

4 Results and discussion

4.1 Inverse modelling of European CH_4 emissions

Figures 1 and 2 show maps of derived CH_4 emissions (average 2006–2007) for inversions S1–CH_4 and S2–CH_4, respectively. Guided by the a priori emission inventory in inversion S1–CH_4, TM5-4DVAR, TM3-STILT and LMDZ-4DVAR largely preserve the "fine structure" of the a priori spatial patterns, but calculate some moderate emission increments on larger regional scales (determined by the chosen spatial correlation scale lengths, ranging between 200 and 600 km). Larger emission increments are apparent for inversion S1–CH_4 of NAME-INV, with generally lower CH_4 emissions across Europe, compared to the a priori and the a posteriori emissions of the other three models.

Inversion S2–CH_4, which is not constrained by a detailed a priori emission inventory, shows in general a smoother spatial distribution than S1–CH_4. While the NAME-INV model does not use any a priori information in S2–CH_4, TM5-4DVAR and TM3-STILT assume that CH_4 emissions are mainly over land. Consequently, NAME-INV attributes much larger emissions over the sea than TM5-4DVAR and TM3-STILT, especially over the North Sea and the Bay of Biscay. All three models show consistently high CH_4 emissions over the Benelux countries and north-western Germany (especially over the highly populated and industrialized Ruhr area). Apart from these hotspot emission areas, TM5-4DVAR and TM3-STILT overall show relatively similar distributions over land, while the NAME-INV inversion differs significantly, for example, over Spain and south-eastern France / north-western Italy, where NAME-INV attributes much lower emissions compared to TM5-4DVAR and TM3-STILT.

It is interesting to compare the inversions S2–CH_4 and the a priori used for S1–CH_4, representing completely independent emission estimates, top-down and bottom-up respectively. Both approaches show coherently elevated CH_4 emissions over Benelux/north-western Germany, and southern UK. The S2–CH_4 inversions also show somewhat elevated emissions per area in southern Poland, where large coal mines are located. However, the inversions are not able to reproduce the very pronounced CH_4 emission hotspot of the bottom-up inventory in this area. This is probably largely due to the limitations of the inversion's ability to resolve point sources accurately (also given the limitation of the sparse atmospheric measurement network) but could also point to a bottom-up overestimate of the CH_4 emissions from the coal mining in this area. In fact, the EDGARv4.2 estimate of CH_4 emissions from coal mines in Poland ($1.71\,\mathrm{Tg\,CH_4\,yr^{-1}}$) is about 4 times higher than that reported under UNFCCC ($0.43\,\mathrm{Tg\,CH_4\,yr^{-1}}$; see Table 6). However, it should be pointed out that the bottom-up emissions have large uncertainties, estimated to be 49 % for UNFCCC, and 83 % for EDGARv4.2 for the coal mines in Poland.

In the following discussion, we analyse the CH_4 emissions per country for the countries whose emissions are reasonably well constrained by the available observations. These are mainly north-western and eastern European countries (Fig. 3), while southern European countries are poorly constrained. For smaller countries, we present aggregated emissions (e.g. Benelux), as they are considered more robust than emissions of individual small countries. The normalized range of derived CH_4 emissions (defined as $(E_{\max} - E_{\min})/(E_{\max} + E_{\min})$) is between ± 16 and ± 44 % for the analysed countries (or combined countries), and ± 25 % for the total CH_4 emissions of all north-western and eastern European countries shown in Fig. 3 (inversion S1–CH_4). For some countries, the range of emission estimates from all four models is close to the uncertainties estimated for the individual inversions (e.g. Poland), but there are also several countries with much larger emission ranges (e.g. France). This shows that there are systematic differences between the inversions, which are not covered by the uncertainty estimates of the individual inversions.

The country totals of the "free" inversion S2–CH_4 are in general very close to those of S1–CH_4 for most countries, demonstrating the strong observational constraints. Apparently, the above-mentioned differences in the smaller-scale "fine structure" in the spatial patterns between S1–CH_4 and S2–CH_4 (see Figs. 1 and 2) are largely compensated by aggregating emissions on the country scale. The fact that in several cases the emission ranges of the S2–CH_4 inversions are smaller than for S1–CH_4 is probably mainly due to fewer models being available (three instead of four).

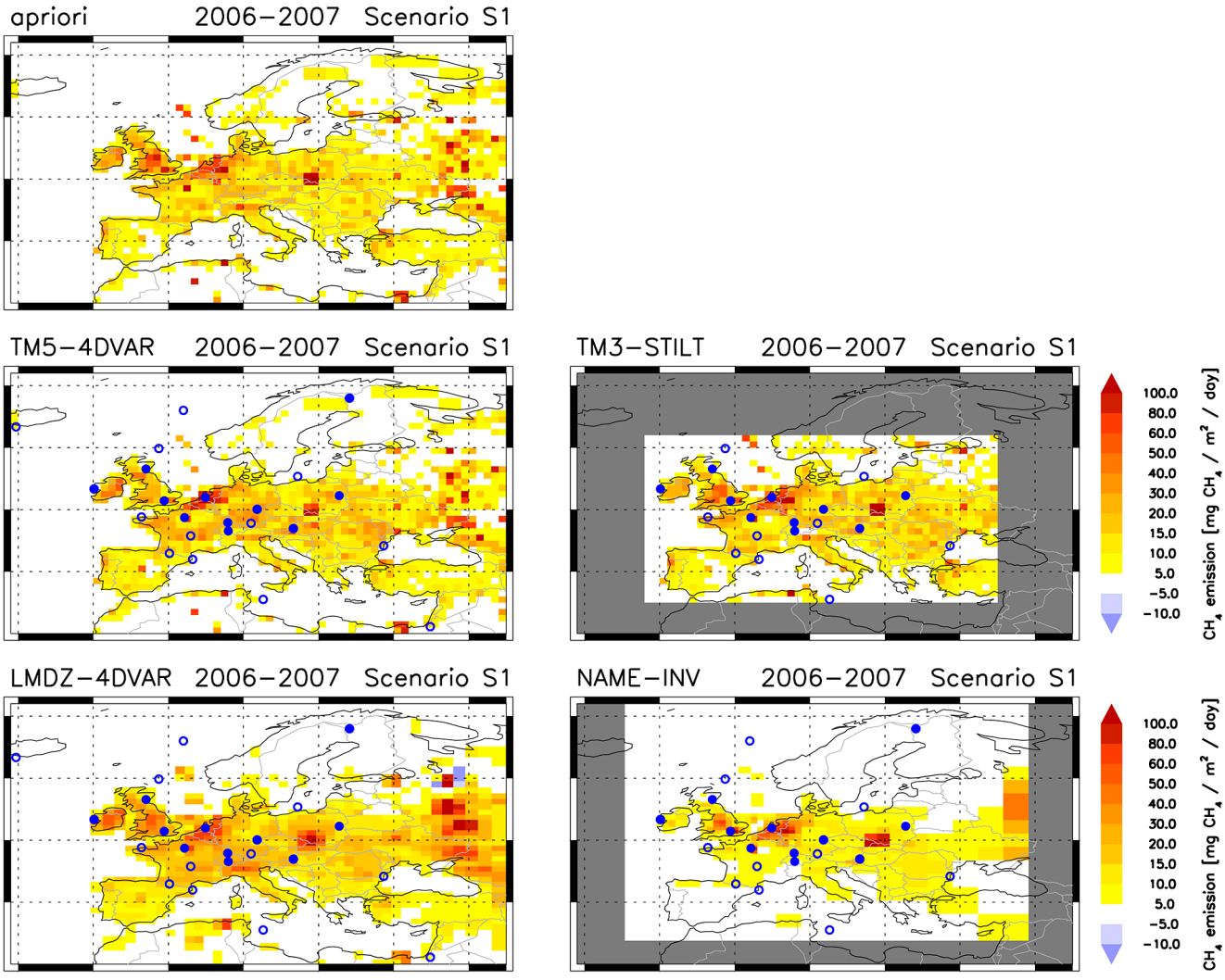

Figure 1. European CH_4 emissions (average 2006–2007, inversion S1–CH_4). Filled circles are measurement stations with quasi-continuous measurements; open circles are discrete air sampling sites.

Table 5. CH_4 and N_2O inversions summary.

Inversion	A priori emission inventory	TM5-4DVAR	LMDZ-4DVAR	TM3-STILT	NAME-INV
CH_4 inversions					
S1–CH_4	As compiled in Table 3	•	•	•	•
S2–CH_4	No a priori	•		•	•
N_2O inversion					
S1–N_2O	As compiled in Table 4	•	•	•	•
S2–N_2O	No a priori	•		•	•

For most countries, the NAME-INV model yields lower emissions compared to the other three models. This is most clearly visible in the total emission of all north-western and eastern European countries, which NAME-INV estimates to be 10.7–11.7 Tg CH_4 yr^{-1} (annual totals for 2006 and 2007, for S1–CH_4 and S2–CH_4), compared to estimates of 16.0–19.4 Tg CH_4 yr^{-1} from TM5-4DVAR, LMDZ-4DVAR and TM3-STILT.

The reasons for the generally lower emissions derived by NAME-INV remain unclear. One factor that may contribute

Table 6. CH_4 emissions from EDGARv4.1, EDGARv4.2, and UNFCCC for major CH_4 source categories. For the UNFCCC emissions, the reported relative uncertainties (2σ) per country and category and corresponding emission ranges are also compiled. Total uncertainties per country (or aggregated countries) are estimated from the reported uncertainties per category assuming no correlation between different UNFCCC categories (but correlated errors for sub-categories). "NWE" is the total of the north-western European countries Germany, France, UK, Ireland and Benelux. "NEE" is the total of the eastern European countries Hungary, Poland, Czech Republic (CZE) and Slovakia (SVK).

			Germany	France	UK + Ireland	Benelux	Hungary	Poland	CZE + SVK	NWE	NEE	NWE + NEE
Solid fuels (1B1)												
Emission (2005)	EDGARv4.1[a]	$Tg\,CH_4\,yr^{-1}$	0.54	0.02	0.14	0.008	0.008	1.69	0.18	0.71	1.88	2.59
Emission (2006–2007)	EDGARv4.2	$Tg\,CH_4\,yr^{-1}$	0.36	0.02	0.08	0.007	0.009	1.71	0.16	0.47	1.87	2.34
Emission (2006–2007)	UNFCCC	$Tg\,CH_4\,yr^{-1}$	0.21	0.01	0.13	0.002	0.001	0.43	0.19	0.35	0.62	0.97
Emission range	UNFCCC	$Tg\,CH_4\,yr^{-1}$	0.13–0.29	N/A[b]	0.11–0.14	0.001–0.002	0.001–0.001	0.22–0.64	0.16–0.21	0.25–0.45	0.38–0.85	0.64–1.30
Relative uncertainty	UNFCCC		37.4 %	N/A[b]	13.0 %	19.8 %	10.4 %	48.6 %	13.2 %	27.8 %	37.9 %	34.2 %
Oil and natural gas (1B2)												
Emission (2005)	EDGARv4.1	$Tg\,CH_4\,yr^{-1}$	0.37	1.44	0.66	0.26	0.08	0.15	0.07	2.73	0.30	3.03
Emission (2006–2007)	EDGARv4.2	$Tg\,CH_4\,yr^{-1}$	0.27	1.49	0.61	0.28	0.08	0.15	0.08	2.64	0.31	2.95
Emission (2006–2007)	UNFCCC	$Tg\,CH_4\,yr^{-1}$	0.28	0.05	0.27	0.06	0.10	0.21	0.07	0.66	0.38	1.03
Emission range	UNFCCC	$Tg\,CH_4\,yr^{-1}$	0.25–0.32	0.04–0.06	0.22–0.32	0.04–0.07	0.05–0.15	0.20–0.22	0.04–0.09	0.55–0.76	0.29–0.46	0.84–1.23
Relative uncertainty	UNFCCC		11.4 %	18.0 %	17.1 %	30.2 %	50.0 %	5.3 %	40.0 %	15.9 %	23.2 %	18.5 %
Enteric fermentation (4A)												
Emission (2005)	EDGARv4.1	$Tg\,CH_4\,yr^{-1}$	1.06	1.39	1.50	0.50	0.09	0.58	0.22	4.45	0.89	5.34
Emission (2006–2007)	EDGARv4.2	$Tg\,CH_4\,yr^{-1}$	1.04	1.37	1.48	0.50	0.09	0.58	0.21	4.40	0.88	5.27
Emission (2006–2007)	UNFCCC	$Tg\,CH_4\,yr^{-1}$	0.99	1.36	1.20	0.48	0.08	0.44	0.14	4.04	0.66	4.70
Emission range	UNFCCC	$Tg\,CH_4\,yr^{-1}$	0.66–1.32	1.15–1.58	0.98–1.42	0.39–0.58	0.07–0.09	0.29–0.59	0.11–0.17	3.17–4.91	0.47–0.85	3.64–5.76
Relative uncertainty	UNFCCC		33.4 %	15.8 %	18.7 %	20.3 %	13.3 %	34.4 %	20.5 %	21.5 %	29.0 %	22.6 %
Manure management (4B)												
Emission (2005)	EDGARv4.1	$Tg\,CH_4\,yr^{-1}$	0.35	0.36	0.25	0.25	0.03	0.15	0.04	1.21	0.21	1.42
Emission (2006–2007)	EDGARv4.2	$Tg\,CH_4\,yr^{-1}$	0.35	0.35	0.25	0.25	0.03	0.14	0.03	1.20	0.20	1.40
Emission (2006–2007)	UNFCCC	$Tg\,CH_4\,yr^{-1}$	0.26	0.48	0.24	0.19	0.07	0.16	0.03	1.17	0.26	1.43
Emission range	UNFCCC	$Tg\,CH_4\,yr^{-1}$	0.18–0.34	0.33–0.62	0.18–0.29	0.04–0.35	0.06–0.09	0.09–0.23	0.02–0.04	0.73–1.61	0.16–0.36	0.89–1.97
Relative uncertainty	UNFCCC		31.3 %	30.4 %	24.9 %	80.4 %	24.0 %	44.6 %	34.0 %	37.8 %	37.7 %	37.8 %
Solid waste disposal on land (6A)												
Emission (2005)	EDGARv4.1	$Tg\,CH_4\,yr^{-1}$	0.60	0.08	1.12	0.35	0.10	0.44	0.08	2.14	0.63	2.76
Emission (2006–2007)	EDGARv4.2	$Tg\,CH_4\,yr^{-1}$	0.51	0.34	1.07	0.28	0.11	0.33	0.15	2.20	0.58	2.78
Emission (2006–2007)	UNFCCC	$Tg\,CH_4\,yr^{-1}$	0.76	0.48	0.84	0.25	0.15	0.39	0.20	2.32	0.73	3.06
Emission range	UNFCCC	$Tg\,CH_4\,yr^{-1}$	0.38–1.14	0.00–0.96	0.44–1.24	0.16–0.34	0.10–0.19	0.04–0.73	0.06–0.35	0.97–3.67	0.20–1.27	1.17–4.94
Relative uncertainty	UNFCCC		50.0 %	102.0 %	47.3 %	36.2 %	31.6 %	89.2 %	71.5 %	58.2 %	72.9 %	61.7 %
Waste water (6B)												
Emission (2005)	EDGARv4.1	$Tg\,CH_4\,yr^{-1}$	0.17	0.19	0.12	0.13	0.03	0.09	0.09	0.60	0.21	0.82
Emission (2006–2007)	EDGARv4.2	$Tg\,CH_4\,yr^{-1}$	0.17	0.19	0,12	0.13	0.03	0.10	0.08	0.60	0.21	0.82
Emission (2006–2007)	UNFCCC	$Tg\,CH_4\,yr^{-1}$	0.01	0.06	0.09	0.01	0.02	0.05	0.04	0.17	0.12	0.28
Emission range	UNFCCC	$Tg\,CH_4\,yr^{-1}$	0.00–0.01	0.00–0.12	0.05–0.13	0.01–0.02	0.02–0.03	0.01–0.09	0.02–0.07	0.05–0.28	0.04–0.19	0.09–0.47
Relative uncertainty	UNFCCC		75.0 %	104.4 %	49.9 %	45.4 %	36.1 %	88.1 %	52.6 %	68.8 %	64.2 %	66.9 %
total												
total major categories	EDGARv4.1	$Tg\,CH_4\,yr^{-1}$	3.08	3.47	3.79	1.49	0.34	3.10	0.68	11.84	4.12	15.96
Total major categories	EDGARv4.2	$Tg\,CH_4\,yr^{-1}$	2.70	3.76	3.60	1.45	0.34	3.01	0.71	11.50	4.06	15.57
Total major categories	UNFCCC	$Tg\,CH_4\,yr^{-1}$	2.51	2.43	2.76	1.00	0.42	1.68	0.67	8.70	2.77	11.47
Total all categories	UNFCCC	$Tg\,CH_4\,yr^{-1}$	2.65	2.56	2.83	1.07	0.43	1.83	0.71	9.11	2.97	12.08
Total uncertainty	UNFCCC	$Tg\,CH_4\,yr^{-1}$	0.52	0.55	0.47	0.21	0.07	0.44	0.15	1.68	0.63	2.27
Relative uncertainty	UNFCCC		20.6 %	22.8 %	16.8 %	20.6 %	17.0 %	26.1 %	22.9 %	19.3 %	22.8 %	19.8 %

[a] Recovery from coal mines not included in EDGARv4.1. [b] Uncertainty of CH_4 emissions from solid fuels in France not available.

is the use of different meteorology in NAME-INV (i.e. meteorology from the Met Office UM) and the other three models (using ECMWF meteorology, albeit different production streams). In sensitivity experiments Manning et al. (2011) found differences of $\sim$ 10–20 % (with different signs for different years) in derived emissions from the UK and north-western Europe, when using ECMWF ERA-Interim instead of Met Office UM meteorology. Hence, differences in the applied meteorological data sets can have a significant impact, but probably explain only part of the differences between NAME-INV and the other models.

In the case of S2–CH_4, the difference in the CH_4 emissions attributed to European countries could be partly due to the higher emissions allocated by NAME-INV to the sea (Figs. 2 and 4). In the absence of any a priori constraint, NAME-INV allocates 4.5–4.9 $Tg\,CH_4\,yr^{-1}$ over the European seas (of which $\sim 1\,Tg\,CH_4\,yr^{-1}$ over the North Sea), while sea emissions are largely suppressed in TM5-4DVAR and TM3-STILT in S2–CH_4 ($< 0.2\,Tg\,CH_4\,yr^{-1}$ over the European seas). In the case of S1–CH_4, the range of CH_4 emissions attributed to the sea by the different models is generally much smaller, 0.6–2.2 $Tg\,CH_4\,yr^{-1}$, due to a priori constraints.

In this study we use the same country mask (from EDGAR) for all models to enable a consistent comparison among all models. This country mask accounts only for emissions over land (in the case of coastal grid-cells, the total emissions of this grid-cell are attributed to the land). In contrast, previous NAME-INV inversion studies used different country masks, taking into account also offshore emissions at some further distance from the coastlines (Manning et al., 2011).

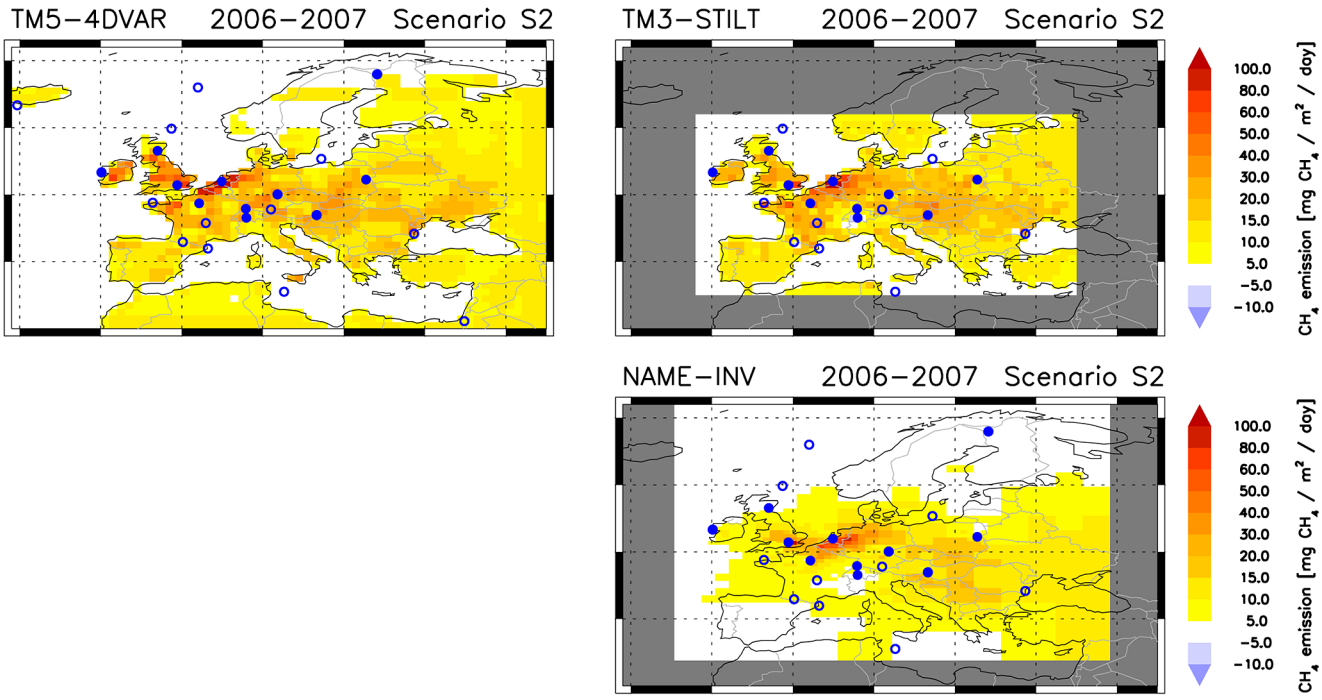

Figure 2. European CH_4 emissions (average 2006–2007, inversion S2–CH_4). Filled circles are measurement stations with quasi-continuous measurements; open circles are discrete air sampling sites.

Table 7. Bias of quasi-continuous N_2O measurements. "CM-FM" denotes the annual average bias between quasi-continuous N_2O measurements and NOAA discrete air samples (using measurements coinciding within 1 h, and the additional condition that the quasi-continuous measurements show low variability (max 0.3 ppb) within a 5 h time window; mean $\pm 1\sigma$ in units of ppb; n: number of coinciding measurements). The columns "TM5–4DVAR" and " LMDZ-4DVAR" give the bias corrections (vs. NOAA flask samples) calculated by the models for inversion S1 (for TM5-4DVAR calculated separately for 2006 and 2007, while LMDZ-4DVAR calculated the average bias over 2006–2007).

Station	CM-FM	TM5-4DVAR	CM-FM	TM5-4DVAR	LMDZ-4DVAR
	2006	2006	2007	2007	2006–2007
PAL	0.50 ± 0.33 ($n = 32$)	0.46	0.31 ± 0.40 ($n = 40$)	0.26	0.53
SIS		0.51		0.64	0.66
TT1		0.86		1.04	0.91
MHD	0.09 ± 0.29 ($n = 28$)	−0.06	0.35 ± 0.53 ($n = 31$)	0.06	0.13
BI5		0.27		0.21	0.19
CB3		0.31		0.59	0.70
OX3	1.07 ($n = 1$)	1.29	0.73 ± 0.21 ($n = 3$)	1.23	1.35
SIL		0.48		0.17	0.54
HU1	0.37 ± 0.83 ($n = 12$)	0.38	0.58 ($n = 1$)	0.39	0.26
JFJ		−0.41		−0.23	−0.26

It is important to note that the inverse modelling estimates the total of the anthropogenic and natural emissions. According to the bottom-up inventories applied in our study, however, it is estimated that natural CH_4 emissions play only a minor role for the countries considered here (shown by the dashed/dotted lines in Figs. 3 and 4). This is important when comparing the CH_4 emissions derived by the inverse models with anthropogenic CH_4 emissions reported to the UNFCCC (shown by black lines in Fig. 3). The range of CH_4 emissions estimated by the inverse models overlaps for most countries with the uncertainty range of the UNFCCC emissions. Nevertheless, there is a clear tendency to higher CH_4 emissions derived by three of the inverse models (TM5-4DVAR, LMDZ-4DVAR, TM3-STILT) compared to UNFCCC, while NAME-INV is in most cases close to UNFCCC. For comparing different approaches, realistic uncertainty estimates are

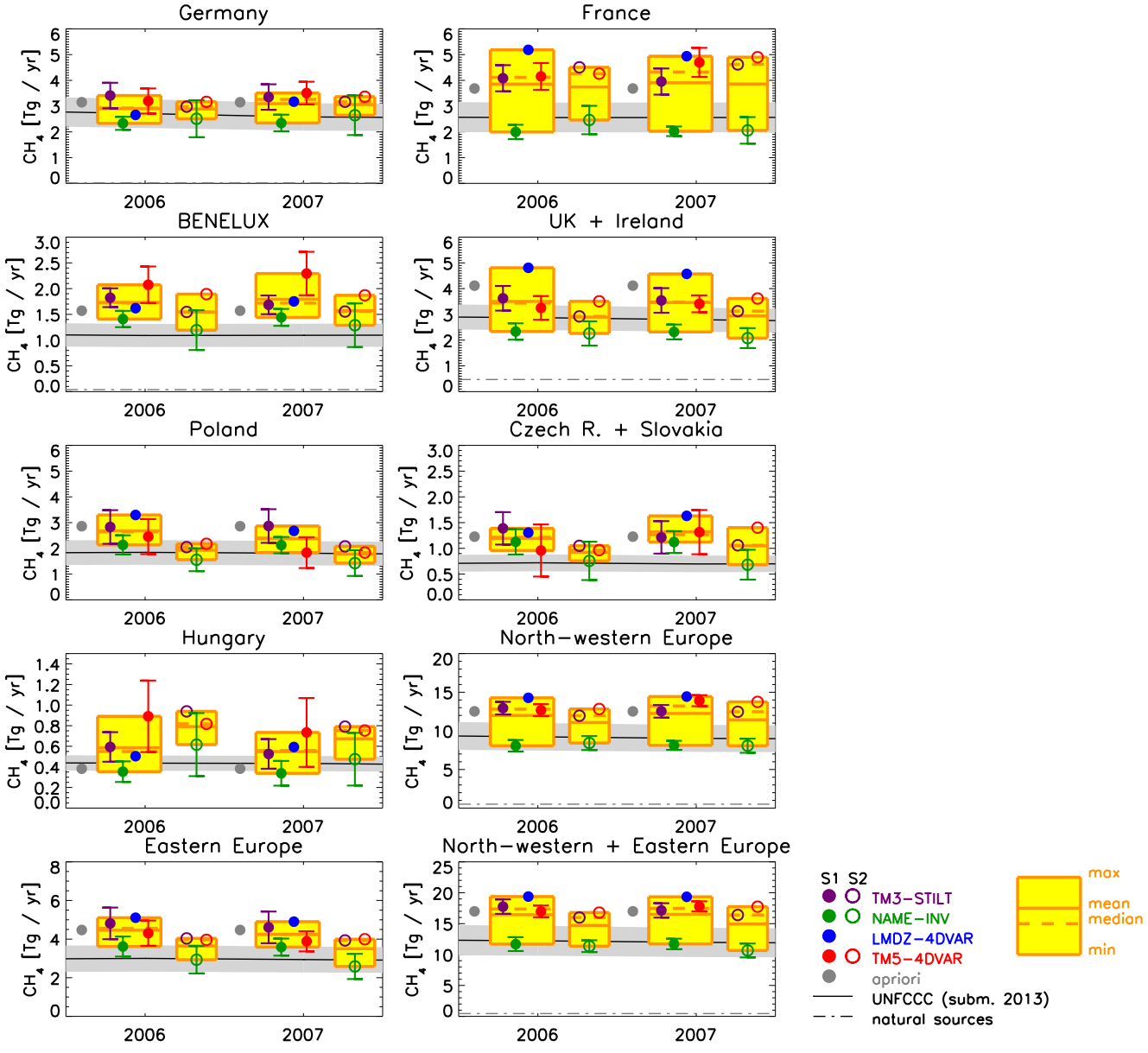

Figure 3. European CH_4 emissions by country and aggregated region. For each year, the left yellow box shows the results for inversion S1–CH_4, and the right yellow box for S2–CH_4. The grey-shaded area is the range of UNFCCC CH_4 emissions (based on reported uncertainties, as compiled in Table 6).

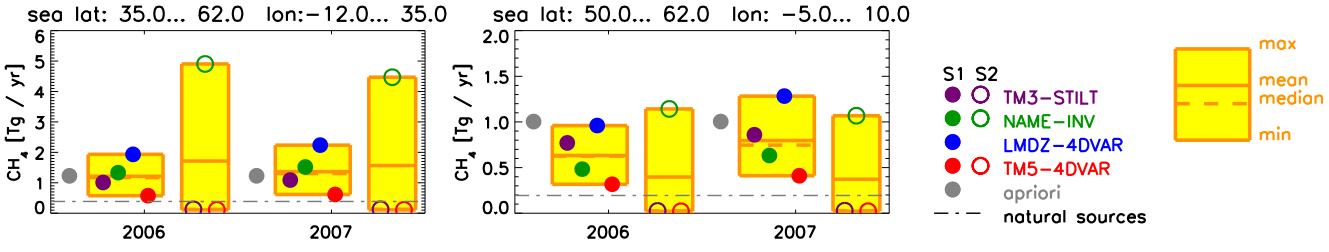

Figure 4. CH_4 emissions over European seas. Left: total CH_4 emissions between 35° and 62° N, and 12° W and 35° E, representing the largest common domain of all models; right: total CH_4 emissions over the North Sea.

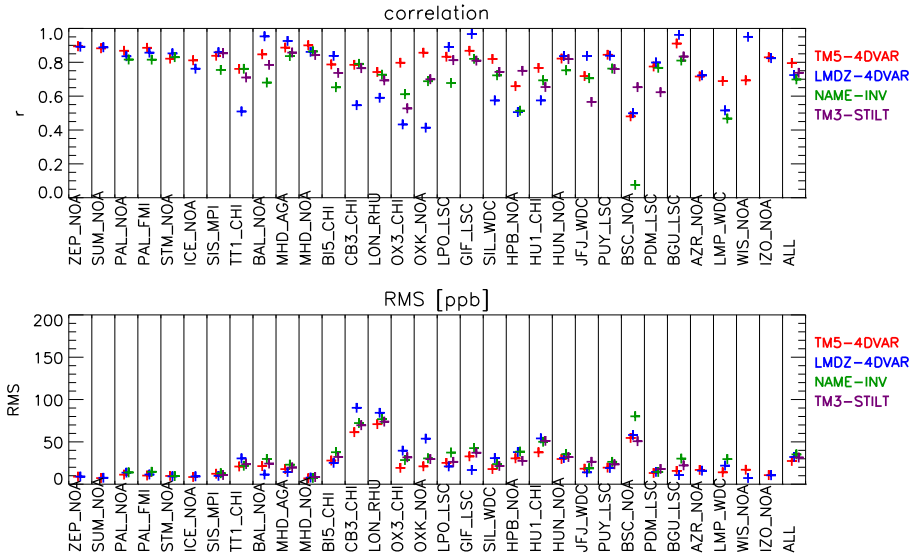

Figure 5. Comparison of modelled and observed CH_4 at stations: correlation coefficients (top) and rms differences (bottom) for inversion S1–CH_4. "All" denotes the mean correlation coefficient and rms difference, averaged over those stations, for which results were available from all models.

essential to evaluate their consistency. Under the UNFCCC, European countries report uncertainty estimates for individual source categories, taking account of uncertainty estimates for activity data and for emission factors (both for CH_4 and for N_2O usually the latter is the dominant term). Since uncertainties of total emissions are usually not reported, we estimate these assuming that the uncertainties of different IPCC/UNFCCC source categories are uncorrelated (but fully correlated for sub-categories). Furthermore, we assume correlated errors when aggregating individual source categories from different countries (as different countries usually apply similar approaches). Table 6 shows the UNFCCC uncertainty estimates for the six major CH_4 source categories and our derived estimates of the total uncertainty per country (and aggregated countries). Overall the estimated total uncertainties are surprisingly low: between 17 and 26 % for the countries considered and about 20 % for the total CH_4 emissions of all north-western and eastern European countries.

Table 6 also includes the CH_4 emission estimates from EDGARv4.1 for 2005 (used as a priori in the inversion) and EDGARv4.2 for 2006–2007 (which became available after completion of the inversions in this study). Overall the numbers for EDGARv4.1 (2005) and EDGARv4.2 for 2006–2007 are very similar (total of north-western and eastern European countries (denoted "NWE + NEE"): 16.0 and 15.6 $Tg\,CH_4\,yr^{-1}$, respectively); smaller differences are due to several updates in EDGARv4.2 and to small trends between 2005 and 2006–2007. Comparison of UNFCCC emissions with EDGARv4.2 shows overall good consistency for enteric fermentation, manure management and solid waste, for which the EDGARv4.2 estimates are for most countries within the uncertainty range of the UNFCCC emissions (Table 6). However, there are considerable differences, in particular for solid fuels (i.e. coal mining) and oil and natural gas, for which EDGARv4.2 estimates 1.4 and 1.9 $Tg\,CH_4\,yr^{-1}$ higher emissions, respectively, for the NWE + NEE total than UNFCCC. For single countries, the largest differences are for solid fuels from Poland (EDGARv4.2: 1.71 (0.29–3.21) $Tg\,CH_4\,yr^{-1}$; UNFCCC: 0.43 (0.22–0.64) $Tg\,CH_4\,yr^{-1}$) and oil and natural gas from France (EDGARv4.2: 1.49 $Tg\,CH_4\,yr^{-1}$; UNFCCC: 0.05 (0.04–0.06) $Tg\,CH_4\,yr^{-1}$). Since uncertainty estimates are not standardly available for each sector and country in EDGARv4.2, a strict comparison cannot be made. However, the large differences between the two bottom-up estimates highlight the large uncertainties for fugitive emissions related to production (and transmission/distribution) of fossil fuels.

For TM5-4DVAR, LMDZ-4DVAR and TM3-STILT, the derived emissions are in general closer to the total emissions from EDGARv4.2 than those from UNFCCC, while NAME-INV, as already mentioned, is relatively close to UNFCCC.

Our inverse modelling estimates of the total emissions per country do not account for offshore emissions. According to EDGARv4.2, about 0.8 $Tg\,CH_4\,yr^{-1}$ is emitted offshore over the European seas (mainly from oil and gas production), while natural CH_4 emissions of about 0.4 $Tg\,CH_4\,yr^{-1}$ over the European seas are estimated from our bottom-up inventories (total between 35° and 62° N and between 12° W and 35° E; see Fig. 4). For comparison, Bange (2006) estimates natural CH_4 emissions from European coastal areas to be in the range 0.5 to 1.0 $Tg\,CH_4\,yr^{-1}$ (including the Arctic Ocean, Baltic Sea, North Sea, northeastern Atlantic Ocean, Mediterranean Sea and Black Sea).

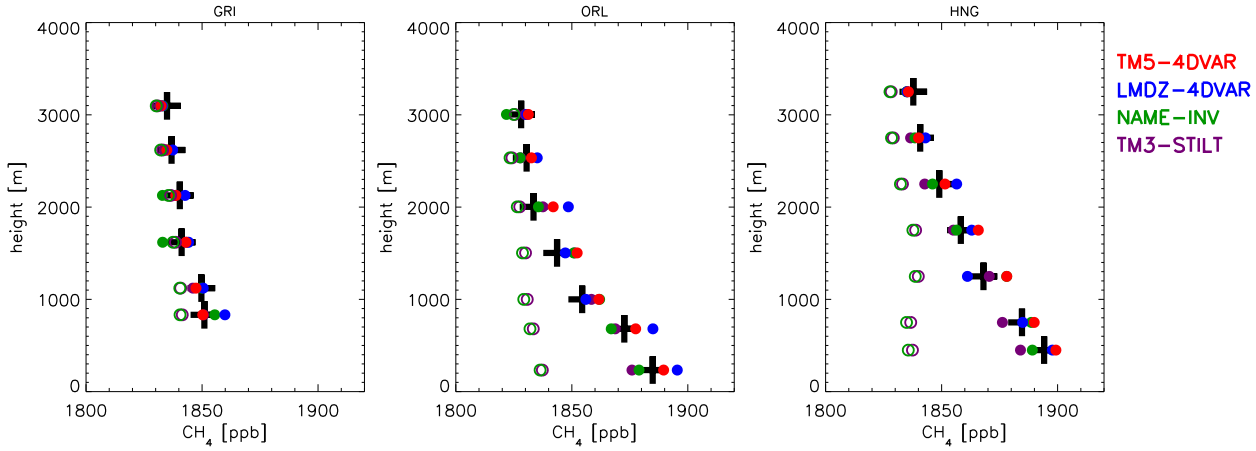

Figure 6. CarboEurope aircraft profile measurements of CH_4 at Griffin (Scotland), Orléans (France) and Hegyhatsal (Hungary) used for validation of atmospheric models. The figure shows the average over all available measurements (black crosses) during 2006–2007 and average of corresponding model simulations (filled coloured symbols; for NAME-INV only a subset of aircraft profiles had been provided). The open circles show the calculated background mixing ratios applied for the limited domain model NAME-INV and STILT, based on the method of Rödenbeck et al. (2009).

The statistics of the assimilated observations are summarized in Fig. 5. Overall, all the models show relatively similar performance, with an average correlation coefficient between 0.7 and 0.8 and an average root mean square (rms) difference between observed and assimilated CH_4 mixing ratios between ~ 25 and ~ 35 ppb.

All models have been validated against regular aircraft profiles performed within the CarboEurope project at three European monitoring sites (Fig. 6). These aircraft data have not been used in the inversion. However, for two aircraft sites (Griffin, Scotland and Hegyhatsal, Hungary) the corresponding surface observations have been assimilated (tall towers Angus (TT1) and Hegyhatsal (HU1)), while the surface observations at Orléans (France) were not used (since they started only in 2007), but the observations from Gif-sur-Yvette, about 100 km north of Orléans, were included. Hence, while surface mixing ratios are well constrained at these three aircraft sites, the comparison of observed and modelled vertical gradients allows the model-simulated vertical transport to be validated, which is of critical importance to the inversions. Figure 6 shows that all models reproduce the average observed vertical gradient in the lower troposphere relatively well, indicating overall realistic vertical mixing.

4.2 Inverse modelling of European N_2O emission

Figures 7 and 8 show maps of derived N_2O emissions (average 2006–2007) for inversions S1–N_2O and S2–N_2O, respectively. European N_2O emissions are dominated by agricultural soils. Furthermore, N_2O emissions from the chemical industry represent strong point sources, which are clearly visible in the a priori emission inventory.

In general, the four models show a relatively consistent picture for S1–N_2O, with moderate N_2O emission increments on larger regional scales, while largely preserving the spatial "fine structure" of the a priori emission inventory. As for S1–CH_4, however, NAME-INV, yields lower N_2O emissions than TM5-4DVAR, LMDZ-4DVAR and TM3-STILT.

In Fig. 8, the three available free N_2O inversions for S2–N_2O consistently show elevated N_2O emissions over Benelux, but none derive the chemical industry hotspots. For S2–N_2O, the N_2O emissions attributed to the sea by NAME-INV are significantly larger (0.26–0.31 Tg N_2O yr^{-1}; Fig. 10) than in S1–N_2O (0.06–0.07 Tg N_2O yr^{-1}), while they remain relatively low in TM5-4DVAR and TM3-STILT (due to the a priori assumption of low emissions over the sea compared to land in these two inversions, which suppresses the attribution of emissions to the sea). Independent studies about N_2O emissions from European seas provide very different estimates. Bange (2006) estimated a net source of N_2O to the atmosphere of 0.33–0.67 Tg N yr^{-1} (equivalent to 0.52–1.05 Tg N_2O yr^{-1}), using measured N_2O saturations of surface waters and air–sea gas exchange rates based on Liss and Merlivat (1986) and Wanninkhof (1992). Bange (2006) attributes the major contribution to estuarine/river systems and not to open shelf areas. In contrast, Barnes and Upstill-Goddard (2011) estimate only 0.007 ± 0.013 Tg N_2O yr^{-1} for European estuarine N_2O emissions, claiming that mean N_2O saturation and mean wind speed for European estuaries might be overestimated in the study of Bange (2006).

Figure 9 shows the total N_2O emissions per country derived by the different inversions, and their comparison with UNFCCC bottom-up inventories. Similar to CH_4, the contribution of natural N_2O emissions (derived from the bottom-up inventories of natural N_2O sources compiled in Table 4)

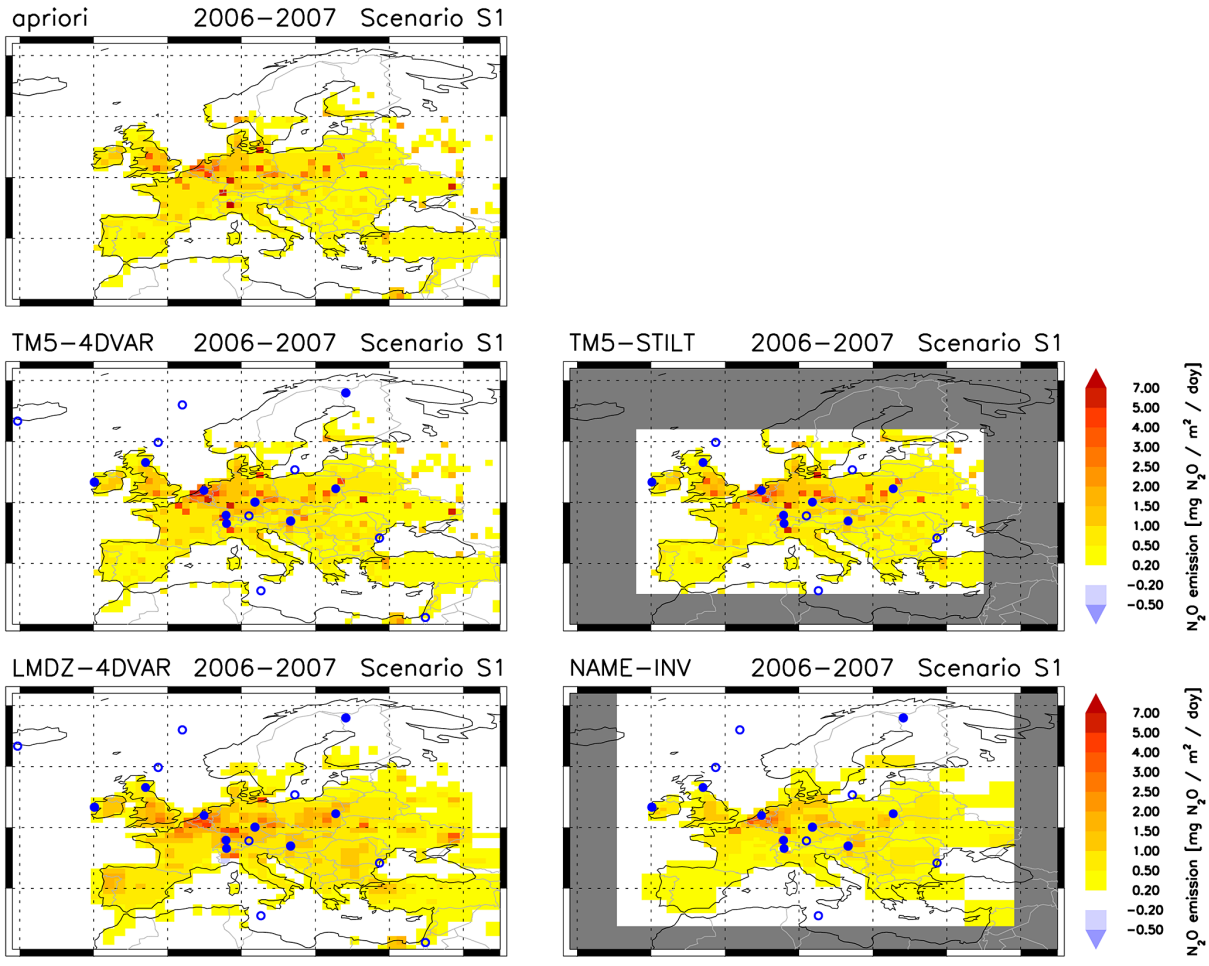

Figure 7. European N_2O emissions (average 2006–2007, inversion S1–N_2O). Filled circles are measurement stations with quasi-continuous measurements, and open circles discrete air sampling sites.

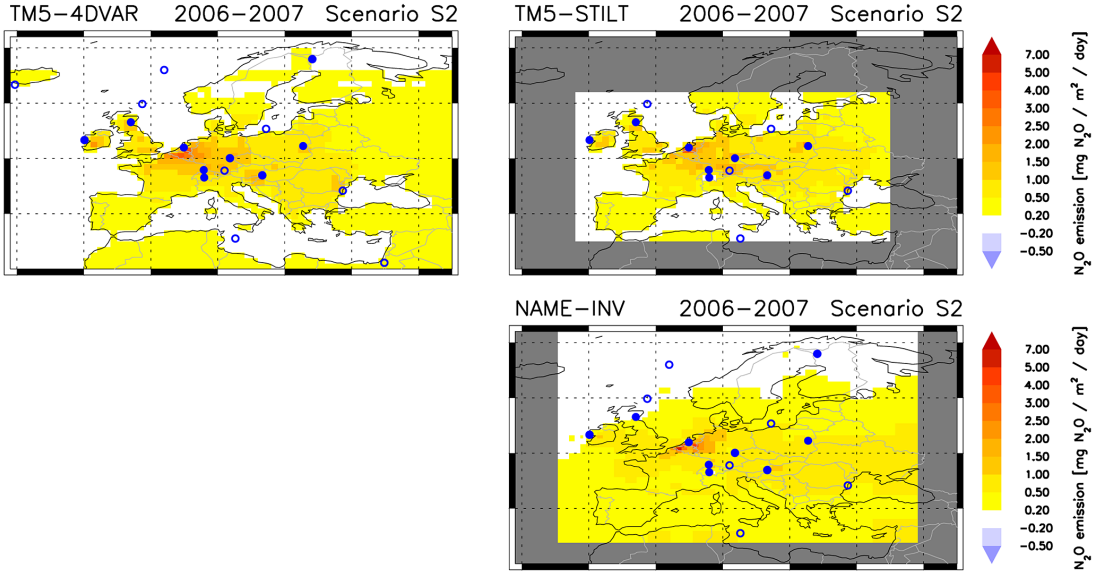

Figure 8. European N_2O emissions (average 2006–2007, inversion S2–N_2O). Filled circles are measurement stations with quasi-continuous measurements, and open circles discrete air sampling sites.

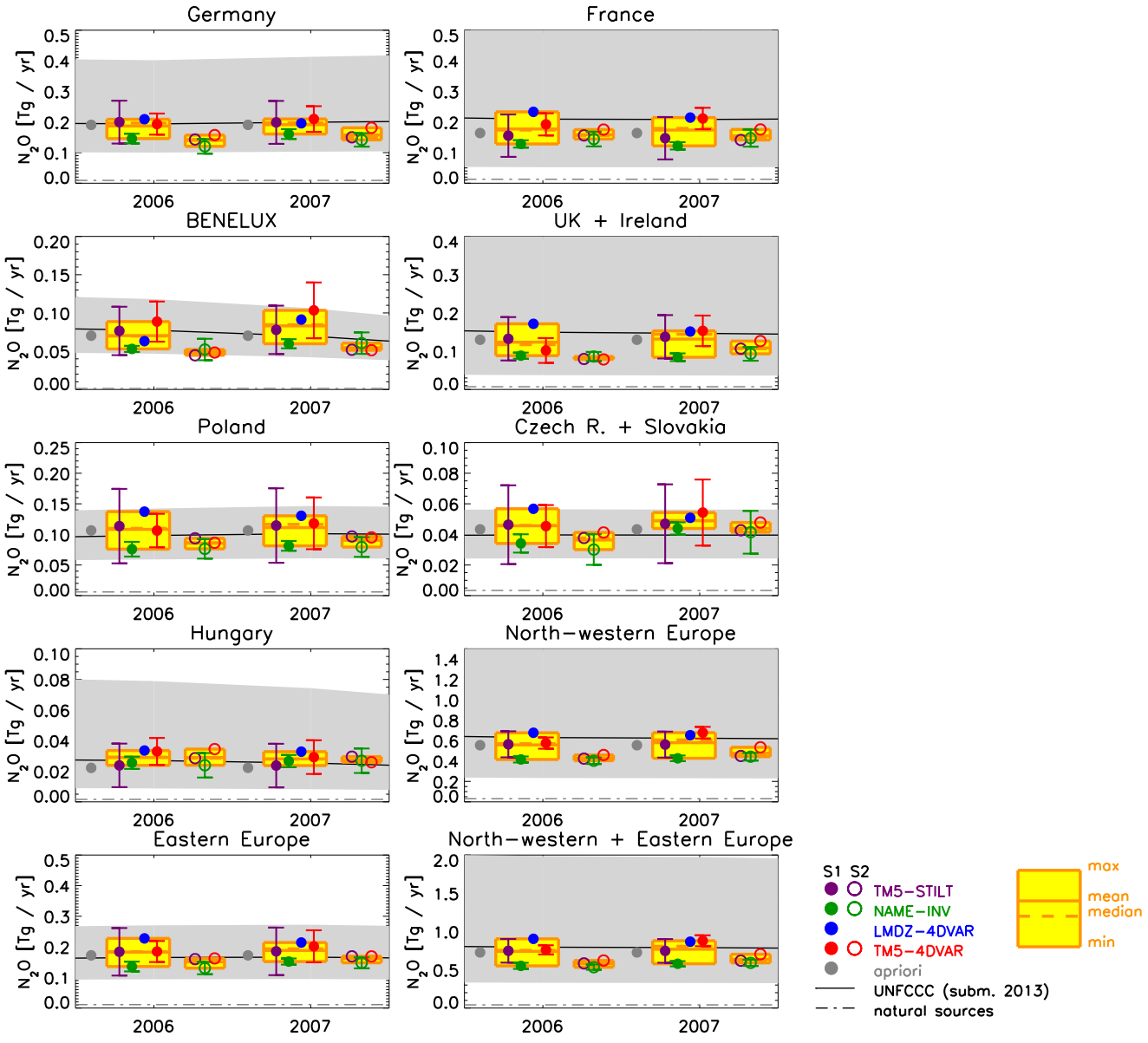

Figure 9. European N_2O emissions by country and aggregated region. For each year, the left yellow box shows the results for inversion S1–N_2O, and the right yellow box for S2–N_2O. The grey-shaded area is the range of UNFCCC N_2O emissions (based on reported uncertainties, as compiled in Table 8; note that for some countries the UNFCCC range exceeds the scale of figures).

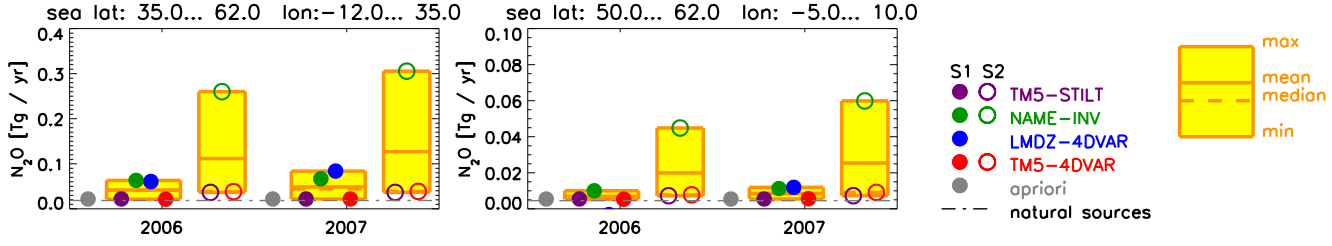

Figure 10. N_2O emissions over European seas. Left: total N_2O emissions between 35° and 62° N, and 12° W and 35° E, representing the largest common domain of all models; right: total N_2O emissions over the North Sea.

Table 8. N_2O emissions from EDGARv4.1, EDGARv4.2 and UNFCCC for major N_2O source categories. For the UNFCCC emissions, the reported relative uncertainties (2σ) per country and category and corresponding emission ranges are also compiled. Total uncertainties per country (or aggregated countries) are estimated from the reported uncertainties per category assuming no correlation between different UNFCCC categories (but correlated errors for sub-categories). "NWE" is the total of the north-western European countries Germany, France, UK, Ireland and Benelux. "NEE" is the total of the eastern European countries Hungary, Poland, Czech Republic (CZE) and Slovakia (SVK).

			Germany	France	UK + Ireland	Benelux	Hungary	Poland	CZE + SVK	NWE	NEE	NWE + NEE
1A Fuel combustion												
Emission (2005)	EDGARv4.1	Tg N_2O yr^{-1}	0.019	0.012	0.010	0.006	0.001	0.013	0.013	0.046	0.026	0.073
Emission (2006–2007)	EDGARv4.2	Tg N_2O yr^{-1}	0.018	0.011	0.010	0.005	0.001	0.012	0.006	0.044	0.020	0.063
Emission (2006–2007)	UNFCCC	Tg N_2O yr^{-1}	0.017	0.015	0.017	0.004	0.001	0.006	0.004	0.052	0.011	0.063
Emission range	UNFCCC	Tg N_2O yr^{-1}	0.012–0.021	0.009–0.021	0.001–0.046	0.001–0.011	0.000–0.001	0.005–0.008	0.001–0.008	0.023–0.098	0.006–0.017	0.029–0.115
Relative uncertainty	UNFCCC		26.2 %	41.2 %	95.3–176.7 %	73.6–162.7 %	71.2 %	22.7 %	76.3 %	56.2–89.3 %	47.1 %	54.6–81.7 %
2B Chemical industry												
Emission (2005)	EDGARv4.1	Tg N_2O yr^{-1}	0.051	0.027	0.015	0.027	0.006	0.020	0.008	0.120	0.034	0.154
Emission (2006–2007)	EDGARv4.2	Tg N_2O yr^{-1}	0.040	0.026	0.017	0.046	0.006	0.024	0.010	0.128	0.040	0.169
Emission (2006–2007)	UNFCCC	Tg N_2O yr^{-1}	0.031	0.019	0.008	0.025	0.004	0.015	0.008	0.083	0.026	0.109
Emission range	UNFCCC	Tg N_2O yr^{-1}	0.027–0.034	0.017–0.021	0.000–0.017	0.019–0.031	0.004–0.004	0.011–0.019	0.007–0.009	0.063–0.103	0.021–0.032	0.084–0.135
Relative uncertainty	UNFCCC		11.1 %	10.2 %	100.0–100.4 %	24.5 %	2.2 %	29.5 %	13.9 %	23.8 %	21.1 %	23.2 %
4B Manure management												
Emission (2005)	EDGARv4.1	Tg N_2O yr^{-1}	0.009	0.008	0.004	0.004	0.001	0.004	0.001	0.025	0.007	0.032
Emission (2006–2007)	EDGARv4.2	Tg N_2O yr^{-1}	0.009	0.008	0.004	0.004	0.001	0.004	0.001	0.025	0.006	0.031
Emission (2006–2007)	UNFCCC	Tg N_2O yr^{-1}	0.009	0.016	0.007	0.006	0.003	0.018	0.004	0.038	0.025	0.063
Emission range	UNFCCC	Tg N_2O yr^{-1}	0.004–0.016	0.008–0.024	0.000–0.033	0.000–0.011	0.000–0.006	0.000–0.045	0.002–0.006	0.012–0.083	0.002–0.057	0.014–0.140
Relative uncertainty	UNFCCC		60.8-69.1 %	50.2 %	100.0–349.6 %	94.4–94.6 %	100.0–100.3 %	100.0–148.9 %	54.7–54.9 %	68.9–119.1 %	93.2–129.2 %	78.5–123.1 %
4D Agricultural soils												
Emission (2005)	EDGARv4.1	Tg N_2O yr^{-1}	0.086	0.098	0.077	0.025	0.012	0.052	0.013	0.285	0.077	0.363
Emission (2006–2007)	EDGARv4.2	Tg N_2O yr^{-1}	0.084	0.096	0.075	0.025	0.012	0.050	0.013	0.280	0.075	0.355
Emission (2006–2007)	UNFCCC	Tg N_2O yr^{-1}	0.129	0.155	0.111	0.035	0.017	0.056	0.022	0.431	0.095	0.525
Emission range	UNFCCC	Tg N_2O yr^{-1}	0.036–0.337	0.000–0.565	0.002–0.509	0.005–0.091	0.000–0.064	0.022–0.091	0.007–0.037	0.043–1.502	0.029–0.193	0.072–1.695
Relative uncertainty	UNFCCC		72.1–160.6 %	100.0–264.9 %	98.1–358.0 %	87.1–158.3 %	100.0–284.2 %	61.5 %	65.7–72.3 %	90.1–248.9 %	69.3–103.3 %	86.3–222.6 %
6B Waste water												
Emission (2005)	EDGARv4.1	Tg N_2O yr^{-1}	0.007	0.006	0.005	0.002	0.001	0.003	0.001	0.020	0.005	0.025
Emission (2006–2007)	EDGARv4.2	Tg N_2O yr^{-1}	0.007	0.006	0.006	0.002	0.001	0.003	0.001	0.020	0.005	0.025
Emission (2006–2007)	UNFCCC	Tg N_2O yr^{-1}	0.008	0.003	0.004	0.002	0.001	0.004	0.001	0.017	0.005	0.023
Emission range	UNFCCC	Tg N_2O yr^{-1}	0.007–0.009	0.000–0.006	0.000–0.020	0.001–0.004	0.000–0.010	0.002–0.005	0.000–0.001	0.008–0.039	0.002–0.017	0.010–0.056
Relative uncertainty	UNFCCC		13.8 %	100.0–104.4 %	91.1–361.1 %	70.8–75.3 %	100.0–1000.0 %	52.2 %	54.4 %	55.2–122.1 %	61.0–218.9 %	56.5–145.0 %
total												
total major categories	EDGARv4.1	Tg N_2O yr^{-1}	0,172	0,150	0,112	0,064	0,021	0,092	0,036	0,497	0,149	0,646
Total major categories	EDGARv4.2	Tg N_2O yr^{-1}	0.158	0.147	0.111	0.082	0.021	0.094	0.031	0.497	0.146	0.643
Total major categories	UNFCCC	Tg N_2O yr^{-1}	0.194	0.207	0.147	0.072	0.025	0.099	0.038	0.621	0.163	0.784
Total all categories	UNFCCC	Tg N_2O yr^{-1}	0.197	0.209	0.148	0.074	0.026	0.100	0.040	0.627	0.166	0.793
Relative uncertainty	UNFCCC		48.3–107.3 %	75.0–198.2 %	75.1–271.3 %	43.9–78.1 %	67.5–192.7 %	39.8–44.6 %	38.6–42.2 %	62.9–173.0 %	43.0–63.8 %	58.5–149.8 %

is estimated to be rather small for the European countries analysed here. Given the large uncertainty of the UNFCCC inventories, the N_2O emissions derived by the inverse models are surprisingly close to the UNFCCC values and the range from all models is well within the UNFCCC uncertainty range for all countries (or aggregated countries). The uncertainty in the UNFCCC emissions is generally dominated by the uncertainty in the N_2O emissions from agricultural soils, for which several countries estimate uncertainties well above 100 % (UK estimate: 424 %). For our estimate of the total uncertainty from the reported uncertainties per category (see Table 8), we take account of the non-symmetric nature of errors above 100 %, assuming zero emissions for the specific category as the lowermost boundary for any relative error larger than 100 %. Figure 9 shows that the range of the inverse modelling estimates is much smaller than the UNFCCC uncertainty range for most countries (including the total emissions from north-western and eastern Europe). This finding is consistent with the analysis of error statistics of bottom-up inventories by Leip (2010), suggesting that the current UNFCCC uncertainty estimates of N_2O bottom-up emission inventories are likely too high.

It is important to note, however, that significant biases in N_2O measurements exist between different laboratories that require corrections (Table 7). The bias corrections calculated by TM5-4DVAR and LMDZ-4DVAR are within ~ 0.3 ppb compared to the bias determined for those stations for which parallel NOAA discrete air measurements are available (for stations with at least 10 coinciding hourly measurements per year). This is somewhat worse than the agreement of 0.1–0.2 ppb reported by Corazza et al. (2011) and may indicate some limitations of the applied bias correction scheme, which does not account for potential changes of the bias within the inversion period (TM5-4DVAR: 1 year, LMDZ-4DVAR: 2 years).

Figure 11 shows the correlation coefficients and rms differences between (bias-corrected) observed and simulated N_2O mixing ratios at the monitoring stations used in inversion S1–N_2O. The mean correlation coefficients for the four models are in the range between 0.6 and 0.7 (averaged over all stations), which is somewhat lower than for CH_4 (average correlation coefficients between 0.7 and 0.8; Fig. 5). This is probably mainly due to the lower atmospheric N_2O variability compared to CH_4, but may be partly also due to the mentioned limitations of the quality of the N_2O data.

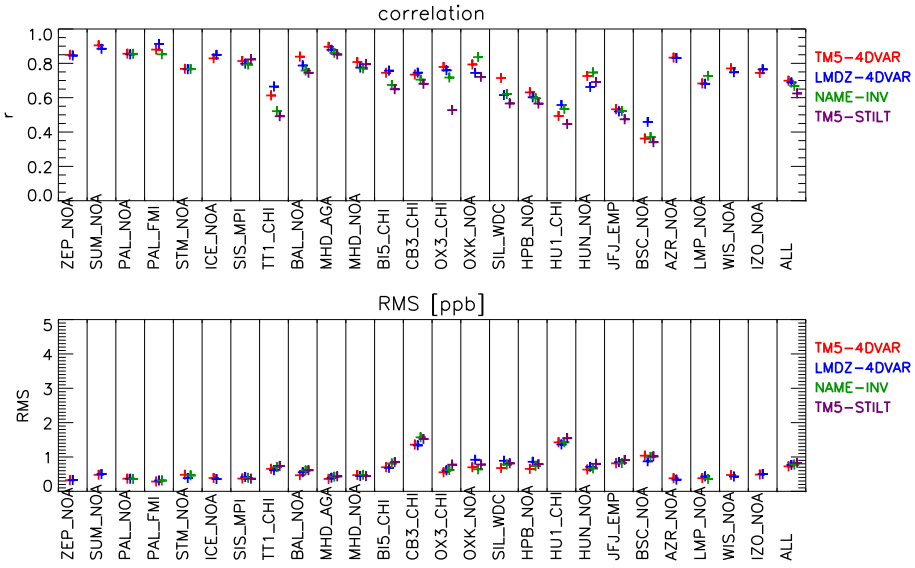

Figure 11. Comparison of modelled and observed N_2O at stations: correlation coefficients (top) and rms differences (bottom) for inversion S1–N_2O (after bias correction of observations). "All" denotes the mean correlation coefficient and rms difference, averaged over the stations for which results were available from all models.

5 Conclusions

We estimated European CH_4 and N_2O emissions for 2006 and 2007 using four different inverse modelling systems that were constrained by quasi-continuous observations from various European monitoring stations (including five tall towers), complemented by further European and global discrete air sampling sites. Although the range of CH_4 emissions estimated by the inverse models overlaps for most countries with the uncertainty range of the UNFCCC emissions, three of four models show a clear tendency to higher emissions compared to the anthropogenic emissions reported under UNFCCC for the total of north-western and eastern European countries (range of TM5-4DVAR, LMDZ-4DVAR and TM3-STILT after correction for natural sources 26–56 % higher than UNFCCC), while NAME-INV yields estimates of country totals very close to UNFCCC. This analysis suggests that (1) CH_4 emissions reported to UNFCCC could be underestimated for some of the European countries analysed in this study, or (2) natural CH_4 emissions are underestimated, or (3) atmospheric models may have significant biases. Although the flux inversions do not allow direct conclusions about specific source categories, the comparison between UNFCCC and EDGARv4.2 shows the critical importance of fugitive emissions from fossil fuels (coal mining, oil production, and production, transmission and distribution of natural gas), for which large differences are apparent between UNFCCC and EDGARv4.2 inventories, outside the estimated UNFCCC uncertainties for some countries. In addition, it is important that natural CH_4 emissions are better quantified in the future, especially CH_4 from wetlands and wet soils. Isotope analysis ($\delta^{13}C$ and δD) could provide some additional information on the relative contribution of different sources; however, the constraints on the European scale might be limited by overlapping isotopic signatures of the sources.

Furthermore, the transport models need better validation. Although the presented validation against independent aircraft CH_4 observations suggests that vertical mixing is realistically modelled overall, we emphasize the need to extend this validation to more sites and to include further diagnostics such as ^{222}Rn and boundary layer height dynamics. These are currently being investigated in more detail in the framework of the InGOS ("Integrated Non-CO_2 Greenhouse Gas Observing System"; http://www.ingos-infrastructure.eu/) project. In addition, it would be useful to include more models in future comparisons to allow more robust estimates of the "inter-model" uncertainties.

The N_2O emissions derived by the inverse models are in general very close to the UNFCCC values, with the range of the inverse modelling estimates being much smaller than the UNFCCC uncertainty range for most countries. This finding suggests that atmospheric observations and inverse modelling can probably constrain N_2O emissions better than bottom-up approaches, and/or that UNFCCC uncertainties (which are dominated by the uncertainties for N_2O emissions from agricultural soils) might be overestimated. However, we emphasize the limitations of the atmospheric N_2O data set used (with biases between different laboratories exceeding the WMO compatibility goal of ± 0.1 ppb), which required significant bias corrections. A major effort is currently being undertaken within the InGOS project to improve and harmonize the European N_2O measurements, which should improve N_2O inversions in the future. A fundamental chal-

lenge for the atmospheric measurements of N_2O, however, remains the generally much lower signal in N_2O compared to CH_4, owing to lower N_2O emissions and the long atmospheric lifetime of N_2O ($\sim$ 130 years compared to $\sim$ 9 years for CH_4, Prather et al., 2012).

This study demonstrates the general feasibility of independent top-down verification of bottom-up inventories. This is particularly important for CH_4 and N_2O because of the large uncertainties (and variability) of emission factors for major CH_4 and N_2O source categories. Future, post-Kyoto international agreements on reductions of GHG emissions would strongly benefit from comprehensive and independent verification to monitor the effectiveness of the emission reduction measures and to ensure the reliability of the reported emissions. However, the application of inverse modelling in this context requires high-quality long-term monitoring of GHGs in the atmosphere with increased density of the monitoring stations, improved atmospheric transport models, and a realistic quantification of uncertainties, in both bottom-up and top-down emission estimates.

Acknowledgements. This work has been supported by the European Commission's Sixth Framework Programme project NitroEurope under Grant Agreement no. 017841-2. The UK Met Office component was equally supported through the Department of Climate Change and Energy contract GA0201. The tall tower observational data were initiated and partially funded by the EU FP5 project CHIOTTO (grant EVK-CT-2002-00163); further data collection and processing were supported by ESF RNP TTorch. We thank Euan Nisbet for helpful comments on the manuscript.

Edited by: M. Shao

References

Aalto, T., Hatakka, J., and Lallo, M.: Tropospheric methane in northern Finland: seasonal variations, transport patterns and correlations with other trace gases, Tellus B, 59, 251–259, 2007.

Athanassiadou, M., Manning, A. J., and Bergamaschi, P.: The NAME-inversion method in the nitro Europe project, in: 14th Conference on Harmonisation within Atmospheric Dispersion Modelling for Regulatory Purposes, 2–6 October 2011, Kos, Greece, available at: http://www.harmo.org/Conferences/Proceedings/_Kos/publishedSections/H14-248.pdf (last access: 13 June 2014), H14–248, 627–631, 2011.

Bange, H. W.: Nitrous oxide and methane in European coastal waters, Estuar. Coast. Shelf S., 70, 361–374, 2006.

Barnes, J. and Upstill-Goddard, R. C.: N_2O seasonal distributions and air–sea exchange in UK estuaries: implications for the tropospheric N_2O source from European coastal waters, J. Geophys. Res., 116, G01006, doi:10.1029/2009JG001156, 2011.

Bergamaschi, P. (Ed.): Atmospheric Monitoring and Inverse Modelling for Verification of National and EU Bottom-up GHG Inventories – report of the workshop "Atmospheric Monitoring and Inverse Modelling for Verification of National and EU Bottom-up GHG Inventories" under the mandate of Climate Change Committee Working Group I, Casa Don Guanella, Ispra, Italy (8–9 March 2007), 153 pp., European Commission Joint Research Centre, Institute for Environment and Sustainability, 2007.

Bergamaschi, P., Frankenberg, C., Meirink, J. F., Krol, M., Dentener, F., Wagner, T., Platt, U., Kaplan, J. O., Körner, S., Heimann, M., Dlugokencky, E. J., and Goede, A.: Satellite chartography of atmospheric methane from SCIAMACHY onboard ENVISAT: 2. Evaluation based on inverse model simulations, J. Geophys. Res., 112, D02304, doi:10.1029/2006JD007268, 2007.

Bergamaschi, P., Frankenberg, C., Meirink, J. F., Krol, M., Villani, M. G., Houweling, S., Dentener, F., Dlugokencky, E. J., Miller, J. B., Gatti, L. V., Engel, A., and Levin, I.: Inverse modeling of global and regional CH_4 emissions using SCIAMACHY satellite retrievals, J. Geophys. Res., 114, D22301, doi:10.1029/2009JD012287, 2009.

Bergamaschi, P., Krol, M., Meirink, J. F., Dentener, F., Segers, A., van Aardenne, J., Monni, S., Vermeulen, A., Schmidt, M., Ramonet, M., Yver, C., Meinhardt, F., Nisbet, E. G., Fisher, R., O'Doherty, S., and Dlugokencky, E. J.: Inverse modeling of European CH_4 emissions 2001–2006, J. Geophys. Res., 115, D22309, doi:10.1029/2010JD014180, 2010.

Bergamaschi, P., Houweling, S., Segers, A., Krol, M., Frankenberg, C., Scheepmaker, R. A., Dlugokencky, E., Wofsy, S., Kort, E., Sweeney, C., Schuck, T., Brenninkmeijer, C., Chen, H., Beck, V., and Gerbig, C.: Atmospheric CH_4 in the first decade of the 21st century: inverse modeling analysis using SCIAMACHY satellite retrievals and NOAA surface measurements, J. Geophys. Res., 118, 7350–7369, doi:10.1002/jgrd.50480, 2013.

Bousquet, P., Ciais, P., Miller, J. B., Dlugokencky, E. J., Hauglustaine, D. A., Prigent, C., Van der Werf, G. R., Peylin, P., Brunke, E.-G., Carouge, C., Langenfelds, R. L., Lathière, J., Papa, F., Ramonet, M., Schmidt, M., Steele, L. P., Tyler, S. C., and White, J.: Contribution of anthropogenic and natural sources to atmospheric methane variability, Nature, 443, 439–443, doi:10.1038/nature05132, 2006.

Bouwman, A. F., Van der Hoek, K. W., and Olivier, J. G. J.: Uncertainties in the global source distribution of nitrous oxide, J. Geophys. Res., 100, 2785–2800, 1995.

Corazza, M., Bergamaschi, P., Vermeulen, A. T., Aalto, T., Haszpra, L., Meinhardt, F., O'Doherty, S., Thompson, R., Moncrieff, J., Popa, E., Steinbacher, M., Jordan, A., Dlugokencky, E., Brühl, C., Krol, M., and Dentener, F.: Inverse modelling of European N_2O emissions: assimilating observations from different networks, Atmos. Chem. Phys., 11, 2381–2398, doi:10.5194/acp-11-2381-2011, 2011.

Cunnold, D. M., Steele, L. P., Fraser, P. J., Simmonds, P. G., Prinn, R. G., Weiss, R. F., Porter, L. W., O'Doherty, S., Langenfelds, R. L., Krummel, P. B., Wang, H. J., Emmons, L., Tie, X. X., Dlugokencky, E. J.: In situ measurements of amospheric methane at GAGE/AGAGE sites during 1985–2000 and resulting inferences, J. Geophys. Res., 107, 4225, doi:10.1029/2001JD001226, 2002.

Dee, D. P., Uppala, S. M., Simmons, A. J., Berrisford, P., Poli, P., Kobayashi, S., Andrae, U., Balmaseda, M. A., Balsamo, G., Bauer, P., Bechtold, P., Beljaars, A. C. M., van de Berg, L., Bidlot, J., Bormann, N., Delsol, C., Dragani, R., Fuentes, M., Geer, A. J., Haimberger, L., Healy, S. B., Hersbach, H., Holm, E. V., Isaksen, L., Kållberg, P., Köhler, M., Matricardi, M., McNally, A. P., Monge-Sanz, B. M., Morcrette, J.-J., Park, B.-K., Peubey,

C., de Rosnay, P., Tavolato, C., Thepaut, J.-N., and Vitart, F.: The ERA-Interim reanalysis: configuration and performance of the data assimilation system, Q. J. Roy. Meteor. Soc., 137, 553–597, 2011.

Dlugokencky, E. J., Steele, L. P., Lang, P. M., and Masarie, K. A.: The growth rate and distribution of atmospheric methane, J. Geophys. Res., 99, 17021–17043, 1994.

Dlugokencky, E. J., Houweling, S., Bruhwiler, L., Masarie, K. A., Lang, P. M., Miller, J. B., and Tans, P. P.: Atmospheric methane levels off: temporary pause or a new steady-state?, Geophys. Res. Lett., 30, 1992, doi:10.1029/2003GL018126, 2003.

Dlugokencky, E. J., Myers, R. C., Lang, P. M., Masarie, K. A., Crotwell, A. M., Thoning, K. W., Hall, B. D., Elkins, J. W., and Steele, L. P.: Conversion of NOAA atmospheric dry air CH_4 mole fractions to a gravimetrically prepared standard scale, J. Geophys. Res., 110, D18306, doi:10.1029/2005JD006035, 2005.

Dlugokencky, E. J., Bruhwiler, L., White, J. W. C., Emmons, L. K., Novelli, P. C., Montzka, S. A., Masarie, K. A., Lang, P. M., Crotwell, A. M., Miller, J. B., and Gatti, L. V.: Observational constraints on recent increases in the atmospheric CH_4 burden, Geophys. Res. Lett., 36, L18803, doi:10.1029/2009GL039780, 2009.

EEA: Annual European Union greenhouse gas inventory 1990–2012 and inventory report 2014, EEA Technical report No. 09/2014, European Commission, DG Climate Action and European Environment Agency, available at: http://www.eea.europa.eu/publications/european-union-greenhouse-gas-inventory-2014, last access: 12 November 2014.

Forster, P., Ramaswamy, V., Artaxo, P., Berntsen, T., Betts, R., Fahey, D. W., Haywood, J., Lean, J., Lowe, D. C., Myhre, G., Nganga, J., Prinn, R., Raga, G., Schulz, M., and Van Dorland, R.: Changes in atmospheric constituents and in radiative forcing, in: Climate Change 2007: The Physical Science Basis. Contribution of Working Group I to the Fourth Assessment Report of the Intergovernmental Panel on Climate Change, edited by: Solomon, S., Qin, D., Manning, M., Chen, Z., Marquis, M., Averyt, K. B., Tignor, M., and Miller, H. L., Cambridge University Press, Cambridge, UK and New York, NY, USA, 2007.

Gerbig, C., Lin, J., Wofsy, S., Daube, B., Andrews, A., Stephens, B., Bakwin, P., and C. Grainger: Toward constraining regional-scale fluxes of CO_2 with atmospheric observations over a continent: 2. Analysis of COBRA data using a receptor-oriented framework, J. Geophys. Res., 108, 4757, doi:10.1029/2003JD003770, 2003.

Gilbert, J. C. and Lemaréchal, C.: Some numerical experiments with variable-storage quasi-Newton algorithms, Mathematical Programming, Math. Programm., 45, 407–435, 1989.

Hall, B. D., Dutton, G. S., and Elkins, J. W.: The NOAA nitrous oxide standard scale for atmospheric observations, J. Geophys. Res., 112, D09305, doi:10.1029/2006JD007954, 2007.

Heimann, M. and Koerner, S.: The Global Atmospheric Tracer Model TM3, Tech. Rep. 5 Rep., Max Planck Institute for Biogeochemistry (MPI-BGC), Jena, Germany, 131 pp., 2003.

Hein, R., Crutzen, P. J., and Heimann, M.: An inverse modeling approach to investigate the global atmospheric methane cycle, Global Biogeochem. Cy., 11, 43–76, 1997.

Hirsch, A. I., Michalak, A. M., Bruhwiler, L. M., Peters, W., Dlugokencky, E. J., and Tans, P. P.: Inverse modeling estimates of the global nitrous oxide surface flux from 1998–2001, Global Biogeochem. Cy., 20, GB1008, doi:10.1029/2004GB002443, 2006.

Hourdin, F. and Armengaud, A.: The use of finite-volume methods for atmospheric advection of trace species, Part I: Test of various formulations in a general circulation model, Mon. Weather Rev., 127, 822–837, 1999.

Hourdin, F., Musat, I., Bony, S., Braconnot, P., Codron, F., Dufresne, J.-L., Fairhead, L., Filiberti, M.-A., Friedlingstein, P., Grandpeix, J.-Y., Krinner, G., Le Van, P., Li, Z.-X., and Lott, F.: The LMDZ4 general circulation model: climate performance and sensitivity to parameterized physics with emphasis on tropical convection, Clim. Dynam., 27, 787–813, 2006.

Houweling, S., Kaminski, T., Dentener, F., Lelieveld, J., and Heimann, M.: Inverse modeling of methane sources and sinks using the adjoint of a global transport model, J. Geophys. Res., 104, 26137–26160, 1999.

Huang, J., Golombek, A., Prinn, R., Weiss, R., Fraser, P., Simmonds, P., Dlugokencky, E. J., Hall, B., Elkins, J., Steele, P., Langenfelds, R., Krummel, P., Dutton, G., and Porter, L.: Estimation of regional emissions of nitrous oxide from 1997 to 2005 using multinetwork measurements, a chemical transport model, and an inverse method, J. Geophys. Res., 113, D17313, doi:10.1029/2007JD009381, 2008.

IPCC: 2006 IPCC Guidelines for National Greenhouse Gas Inventories, Prepared by the National Greenhouse Gas Inventories Programme Institute for Global Environmental Strategies, Japan, available at: http://www.ipcc-nggip.iges.or.jp/public/2006gl/pdf/0_Overview/V0_0_Cover.pdf (last access: 13 June 2014), 2006.

Jones, A. R., Thomson, D. J., Hort, M., and Devenish, B.: The U. K. Met Office's next-generation atmospheric dispersion model, NAME III, in: Proceedings of the 27th NATO/CCMS International Technical Meeting on Air Pollution Modelling and its Application, edited by: Borrego, C. and Norman, A. L., 580–589, Springer, available at: http://link.springer.com/chapter/10.1007/978-0-387-68854-1_62#page-2 (last access: 13 June 2014), 2007.

Karion, A., Sweeney, C., Pétron, G., Frost, G., Hardesty, R. M., Kofler, J., Miller, B. R., Newberger, T., Wolter, S., Banta, R., Brewer, A., Dlugokencky, E., Lang, P. M., Montzka, S. A., Schnell, R., Tans, P., Trainer, M., Zamora, R., and Conley, S.: Methane emissions estimate from airborne measurements over a western United States natural gas field, Geophys. Res. Lett., 40, 1–5, 2013.

Kirschke, S., Bousquet, P., Ciais, P., Saunois, M., Canadell, J. G., Dlugokencky, E. J., Bergamaschi, P., Bergmann, D., Blake, D. R., Bruhwiler, L., Cameron-Smith, P., Castaldi, S., Chevallier, F., Feng, L., Fraser, A., Heimann, M., Hodson, E. L., Houweling, S., Josse, B., Fraser, P. J., Krummel, P. B., Lamarque, J.-F., Langenfelds, R. L., Le Quéré, C., Naik, V., O'Doherty, S., Palmer, P. I., Pison, I., Plummer, D., Poulter, B., Prinn, R. J., Rigby, M., Ringeval, B., Santini, M., Schmidt, M., Shindell, D. T., Simpson, I. J., Spahni, R., Steele, L. P., Strode, S. A., Sudo, K., Szopa, S., van der Werf, G. R., Voulgarakis, A., van Weele, M., Weiss, R. F., Williams, J. E., and Zeng, G.: Three decades of global methane sources and sinks, Nat. Geosci., 6, 813–823, 2013.

Kort, E. A., Eluszkiewicz, J., Stephens, B. B., Miller, J. B., Gerbig, C., Nehrkorn, T., D. B. C., Kaplan, J. O., Houweling, S., and Wofsy, S. C.: Emissions of CH_4 and N_2O over the United States and Canada based on a receptor-oriented modeling frame-

work and COBRA-NA atmospheric observations, Geophys. Res. Lett., 35, L18808, doi:10.1029/2008GL034031, 2008.

Krol, M., Houweling, S., Bregman, B., van den Broek, M., Segers, A., van Velthoven, P., Peters, W., Dentener, F., and Bergamaschi, P.: The two-way nested global chemistry-transport zoom model TM5: algorithm and applications, Atmos. Chem. Phys., 5, 417–432, doi:10.5194/acp-5-417-2005, 2005.

Lambert, G. and Schmidt, S.: Reevaluation of the oceanic flux of methane: uncertainties and long term variations, Chemosphere, 26, 579–589, 1993.

Leip, A.: Quantitative quality assessment of the greenhouse gas inventory for agriculture in Europe, Climatic Change, 103, 245–261, 2010.

Leip, A., Busto, M., Corazza, M., Bergamaschi, P., Koeble, R., Dechow, R., Monni, S., and de Vries, W.: Estimation of N_2O fluxes at the regional scale: data, models, challenges, Current Opinion in Environmental Sustainability, 3, 1–11, 2011.

Lin, J. C., Gerbig, C., Wofsy, S. C., Andrews, A. E., Daube, B. C., Davis, K. J., and Grainger, C. A.: A near-field tool for simulating the upstream influence of atmospheric observations: the Stochastic Time-Inverted Lagrangian Transport (STILT) model, J. Geophys. Res., 108, 4493, doi:10.1029/2002JD003161, 2003.

Liss, P. S. and Merlivat, L.: Air–sea exchange rates: introduction and synthesis, in: The Role of Air–Sea Exchange in Geochemical Cycling, edited by: Buat-Menard, P., Reidel Publishing Company, Dordrecht, 113–127, 1986.

Manning, A. J., O'Doherty, S., Jones, A. R., Simmonds, P. G., and Derwent, R. G.: Estimating UK methane and nitrous oxide emissions from 1990 to 2007 using an inversion modeling approach, J. Geophys. Res., 116, D02305, doi:10.1029/2010JD014763, 2011.

Meirink, J. F., Bergamaschi, P., and Krol, M. C.: Four-dimensional variational data assimilation for inverse modelling of atmospheric methane emissions: method and comparison with synthesis inversion, Atmos. Chem. Phys., 8, 6341–6353, doi:10.5194/acp-8-6341-2008, 2008.

Mikaloff Fletcher, S. E., Tans, P. P., Bruhwiler, L. M., Miller, J. B., and Heimann, M.: CH_4 sources estimated from atmospheric observations of CH_4 and its $^{13}C/^{12}C$ isotopic ratios: 2. Inverse modelling of CH_4 fluxes from geographical regions, Global Biogeochem. Cy., 18, GB4005, doi:10.1029/2004GB002224, 2004a.

Mikaloff Fletcher, S. E., Tans, P. P., Bruhwiler, L. M., Miller, J. B., and Heimann, M.: CH_4 sources estimated from atmospheric observations of CH_4 and its $^{13}C/^{12}C$ isotopic ratios: 1. Inverse modelling of source processes, Global Biogeochem. Cy., 18, GB4004, doi:10.1029/2004GB002223, 2004b.

Miller, S. M., Wofsy, S. C., Michalak, A. M., Kort, E. A., Andrews, A. E., Biraud, S. C. , Dlugokencky, E. J. , Eluszkiewicz, J., Fischer, M. L. , Janssens-Maenhout, G., Miller, B. R. , Miller, J. B. , Montzka, S. A. , Nehrkorn, T., and Sweeney, C.: Anthropogenic emissions of methane in the United States, Proc. Natl. Acad. Sci. USA, 110, 20018–20022, doi:10.1073/pnas.1314392110, 2013.

Myhre, G., Shindell, D., Bréon, F.-M., Collins, W., Fuglestvedt, J., Huang, J., Koch, D., Lamarque, J.-F., Lee, D., Mendoza, B., Nakajima, T., Robock, A., Stephens, G., Takemura, T., and Zhang, H.: Anthropogenic and Natural Radiative Forcing, in Climate Change 2013: The Physical Science Basis. Contribution of Working Group I to the Fifth Assessment Report of the Intergovernmental Panel on Climate Change, edited by: Stocker, T. F., Qin, D., Plattner, G.-K., Tignor, M., Allen, S. K., Boschung, J., Nauels, A., Xia, Y., Bex, V., and Midgley, P. M., Cambridge University Press, Cambridge, UK and New York, NY, USA, 659–740, 2013.

Peylin, P., Law, R. M., Gurney, K. R., Chevallier, F., Jacobson, A. R., Maki, T., Niwa, Y., Patra, P. K., Peters, W., Rayner, P. J., Rödenbeck, C., van der Laan-Luijkx, I. T., and Zhang, X.: Global atmospheric carbon budget: results from an ensemble of atmospheric CO_2 inversions, Biogeosciences, 10, 6699–6720, doi:10.5194/bg-10-6699-2013, 2013.

Pison, I., Bousquet, P., Chevallier, F., Szopa, S., and Hauglustaine, D.: Multi-species inversion of CH_4, CO and H_2 emissions from surface measurements, Atmos. Chem. Phys., 9, 5281–5297, doi:10.5194/acp-9-5281-2009, 2009.

Pison, I., Ringeval, B., Bousquet, P., Prigent, C., and Papa, F.: Stable atmospheric methane in the 2000s: key-role of emissions from natural wetlands, Atmos. Chem. Phys., 13, 11609–11623, doi:10.5194/acp-13-11609-2013, 2013.

Popa, M. E., Gloor, M., Manning, A. C., Jordan, A., Schultz, U., Haensel, F., Seifert, T., and Heimann, M.: Measurements of greenhouse gases and related tracers at Bialystok tall tower station in Poland, Atmos. Meas. Tech., 3, 407–427, doi:10.5194/amt-3-407-2010, 2010.

Prather, M. J., Holmes, C. D., and Hsu, J.: Reactive greenhouse gas scenarios: systematic exploration of uncertainties and the role of atmospheric chemistry, Geophys. Res. Lett., 39, L09803, doi:10.1029/2012GL051440, 2012.

Prinn, R. G., Weiss, R. F., Fraser, P. J., Simmonds, P. G., Cunnold, D. M., Alyea, F. N., O'Doherty, S., Salameh, P., Miller, B. R., Huang, J., Wang, R. H. J., Hartley, D. E., Harth, C., Steele, L. P., Sturrock, G., Midgely, P. M., and McCulloch, A.: A history of chemically and radiatively important gases in air deduced from ALE/GAGE/AGAGE, J. Geophys. Res., 115, 17751–17792, 2000.

Ravishankara, A. R., Daniel, J. S., and Portmann, R. W.: Nitrous oxide (N_2O): the dominant ozone-depleting substance emitted in the 21st century, Science, 326, 123–125, 2009.

Ridgwell, A. J., Marshall, S. J., and Gregson, K.: Consumption of atmospheric methane by soils: a process-based model, Global Biogeochem. Cy., 13, 59–70, doi:10.1029/1998GB900004, 1999.

Rigby, M., Prinn, R. G., Fraser, P. J., Simmonds, P. G., Langenfelds, R. L., Huang, J., Cunnold, D. M., Steele, L. P., Krummel, P. B., Weiss, R. F., O'Doherty, S., Salameh, P. K., Wang, H. J., Harth, C. M., Mühle, J., and Porter, L. W.: Renewed growth of atmospheric methane, Geophys. Res. Lett., 35, L22805, doi:10.1029/2008GL036037, 2008.

Rödenbeck, C.: Estimating CO_2 sources and sinks from atmospheric mixing ratio measurements using a global inversion of atmospheric transport, Tech. Rep. 6, Max-Planck-Institut für Biogeochemie, Jena, available at: http://www.bgc-jena.mpg.de/uploads/Publications/TechnicalReports/tech_report6.pdf (last access: 13 June 2014), Max-Planck-Institut für Biogeochemie, Jena, Germany, 2005.

Rödenbeck, C., Houweling, S., Gloor, M., and Heimann, M.: CO_2 flux history 1982–2001 inferred from atmospheric data using a global inversion of atmospheric transport, Atmos. Chem. Phys., 3, 1919–1964, doi:10.5194/acp-3-1919-2003, 2003.

Rödenbeck, C., Gerbig, C., Trusilova, K., and Heimann, M.: A two-step scheme for high-resolution regional atmospheric trace gas inversions based on independent models, Atmos. Chem. Phys., 9, 5331–5342, doi:10.5194/acp-9-5331-2009, 2009.

Sanderson, M. G.: Biomass of termites and their emissions of methane and carbon dioxide: a global database, Global Biogeochem. Cy., 10, 543–557, 1996.

Schmidt, M., Ramonet, M., Wastine, B., Delmotte, M., Galdemard, P., Kazan, V., Messager, C., Royer, A., Valant, C., Xueref, I., and Ciais, P.: RAMCES: the French network of atmospheric greenhouse gas monitoring, in: 13th WMO/IAEA Meeting of Experts on Carbon Dioxide Concentration and Related Tracers Measurement Techniques, WMO report 168, Boulder, Colorado, USA, 19–22 September 2005, 165–174, 2006.

Shindell, D. T., Faluvegi, G., Bell, N., and Schmidt, G.: An emissions-based view of climate forcing by methane and tropospheric ozone, Geophys. Res. Lett., 32, L04803, doi:10.1029/2004GL021900, 2005.

Stephens, B. B., Gurney, K. R., Tans, P. P., Sweeney, C., Peters, W., Bruhwiler, L., Ciais, P., Ramonet, M., Bousquet, P., Nakazawa, T., Aoki, S., Machida, T., Inoue, G., Vinnichenko, N., Lloyd, J., Jordan, A., Heimann, M., Shibistova, O., Langenfelds, R. L., Steele, L. P., Francey, R. J., and Denning, A. S.: Weak northern and strong tropical land carbon uptake from vertical profiles of atmospheric CO_2, Science, 316, 1732–1735, 2007.

Thompson, R. L., Manning, A. C., Gloor, E., Schultz, U., Seifert, T., Hänsel, F., Jordan, A., and Heimann, M.: In-situ measurements of oxygen, carbon monoxide and greenhouse gases from Ochsenkopf tall tower in Germany, Atmos. Meas. Tech., 2, 573–591, doi:10.5194/amt-2-573-2009, 2009.

Thompson, R. L., Bousquet, P., Chevallier, F., Rayner, P. J., and Ciais, P.: Impact of the atmospheric sink and vertical mixing on nitrous oxide fluxes estimated using inversion methods, J. Geophys. Res., 116, D17307, doi:10.1029/2011JD015815, 2011.

Thompson, R. L., Ishijima, K., Saikawa, E., Corazza, M., Karstens, U., Patra, P. K., Bergamaschi, P., Chevallier, F., Dlugokencky, E., Prinn, R. G., Weiss, R. F., O'Doherty, S., Fraser, P. J., Steele, L. P., Krummel, P. B., Vermeulen, A., Tohjima, Y., Jordan, A., Haszpra, L., Steinbacher, M., Van der Laan, S., Aalto, T., Meinhardt, F., Popa, M. E., Moncrieff, J., and Bousquet, P.: TransCom N_2O model inter-comparison – Part 2: Atmospheric inversion estimates of N_2O emissions, Atmos. Chem. Phys., 14, 6177–6194, doi:10.5194/acp-14-6177-2014, 2014.

Trusilova, K., Rödenbeck, C., Gerbig, C., and Heimann, M.: Technical Note: A new coupled system for global-to-regional downscaling of CO_2 concentration estimation, Atmos. Chem. Phys., 10, 3205–3213, doi:10.5194/acp-10-3205-2010, 2010.

van der Werf, G. R., Randerson, J. T., Collatz, G. J., Giglio, L., Kasibhatla, P. S., Arellano Jr., A. F., Olsen, S. C., and Kasischke, E. S.: Continental-Scale Partitioning of Fire Emissions During the 1997 to 2001 El Nino/LaNina Period, Science, 303, 73–76, 2004.

Vermeulen, A. T., Schmidt, M., Manning, A., Moors, E., Moncrieff, J., Haszpra, L., Stefani, P., and Lindroth, A.: CHIOTTO, Final Report Rep. ECN-E–07-052, 118 pp., ECN, Petten, 2007.

Vermeulen, A. T., Hensen, A., Popa, M. E., van den Bulk, W. C. M., and Jongejan, P. A. C.: Greenhouse gas observations from Cabauw Tall Tower (1992–2010), Atmos. Meas. Tech., 4, 617–644, doi:10.5194/amt-4-617-2011, 2011.

Wanninkhof, R.: Relationship between wind speed and gas exchange over the ocean, J. Geophys. Res., 97, 7373–7382, 1992.

WMO: 16th WMO/IAEA Meeting on Carbon Dioxide, Other Greenhouse gases, and Related Measurement Techniques (Wellington, New Zealand, 25–28 October 2011), GAW Report No. 206 Rep., Geneva, Switzerland, 72 pp., 2012.

WMO: WMO greenhouse gas bulletin – The State of Greenhouse Gases in the Atmosphere Based on Global Observations through 2012 Rep., 4 pp., World Meteorological Organization, Geneva, 2013.